REPORT DOCUMENTATION PAGE

AFRL-SR-BL-TR-99-

0012

1. AGENCY USE ONLY *(Leave Blank)*	2. REPORT DATE	3. REPORT TYPE AND DATES COVERED
	December 1, 1998	Final Technical Report 06 Jan 97 - 30 Nov 98

4. TITLE AND SUBTITLE

Advanced Synthesis of Carbon Nitride

5. FUNDING NUMBERS

F49620-97-C0023
2303/ES
61102F

4. AUTHOR(S)

D. J. Benard

7. PERFORMING ORGANIZATION NAME(S) AND ADDRESS(ES)

ROCKWELL SCIENCE CENTER, LLC
1049 CAMINO DOS RIOS
THOUSAND OAKS, CA 91360

7. PERFORMING ORGANIZATION REPORT NUMBER

SC71133.FTR

9. SPONSORING / MONITORING AGENCY NAME(S) AND ADDRESS(ES)

Air Force Office of Scientific Research
Directorate of Chemical and Atmospheric Sciences
801 N. Randolph Street, Room 732
Arlington, VA 22203-1977

9. SPONSORING / MONITORING AGENCY REPORT NUMBER

11. SUPPLEMENTARY NOTES

DISTRIBUTION STATEMENT A
Approved for public release;
Distribution Unlimited

12a. DISTRIBUTING/AVAILABILITY STATEMENT

Approved for public release;
distribution unlimited.

12b. DISTRIBUTION CODE

19990126 051

13. ABSTRACT *(Maximum 200 Words)*

Thin films composed of carbon and nitrogen were generated on a variety of substrates by deposition of radicals obtained after dissociation of gaseous cyanogen azide or solid cyanuric triazide (CTA). These intermediates were obtained upon reacting cyanogen halides or cyanuric chloride, respectively, with sodium azide. The CTA was chemically pure, whereas the gaseous azides were contaminated by halogens that were difficult to safely remove. Energy transfer from discharged nitrogen in a low-pressure flowtube reactor was used to dissociate cyanogen azide and ultraviolet photolysis was employed at ambient pressure to dissociate CTA. Films generated at low pressure demonstrated a bandgap of 2.6 eV with a 2.3 refractive index at visible wavelength. X-ray photoelectron spectroscopy showed the films to consist of near equal yields of diamond-like carbon and a phase with carbon nitride stoichiometry. Films from both donors demonstrated absorption bands in the infrared that peaked at 1600 and 3150 wave numbers. Film adhesion was best on silicon carbide and aluminum nitride, on substrates that were heated during deposition, and when made from CTA. Deposition onto silicon carbide or aluminum nitride at 360°C yielded crystalline films with x-ray diffraction peaks that precisely matched the known ultrahard beta-phase of carbon nitride.

14. SUBJECT TERMS	15. NUMBER OF PAGES
Carbon Nitride, Cyanogen Azide, Cyanuric Triazide, Synthesis, Film Adhesion, Optical and Electrical Properties, X-ray Diffraction and Photoelectron Emission, Visible and Infrared Spectroscopy	35
	16. PRICE CODE

17. SECURITY CLASSIFICATION OF REPORT	18. SECURITY CLASSIFICATION OF THIS PAGE	19. SECURITY CLASSIFICATION OF ABSTRACT	20. LIMITATION OF ABSTRACT
UNCLASSIFIED	UNCLASSIFIED	UNCLASSIFIED	Unlimited

Table of Contents

INTRODUCTION

Background / Program Objectives

In recent years, the search for ultra-hard materials has been aided by ab initio or first principle calculations that determine the minimum energy configuration of a chemical system and its variation with density or lattice parameter. In particular, the search for a material harder than natural diamond has lead to both a theoretical and experimental focus on a proposed beta-phase of carbon nitride (analogous to the known beta-phase of silicon nitride). In principle, this covalent metastable material would have C_3N_4 stoichiometry, no direct C-C or N-N bonds, hardness greater than natural diamond and an extremely wide optical transparency range. Owing to the great utility such a material would have in numerous DoD and commercial applications, a wide variety of experimental methods have been investigated over the last decade as potential synthetic routes to its generation. The work reported here is principally motivated by the possibility of developing area scalable, low-cost and hard abrasion resistant coatings. These coatings are important to the DoD to prolong the useful life of soft infrared window materials in hostile environments.

Numerous physical methods using a wide variety of source technologies for the synthesis of beta-C_3N_4 have been attempted in which C and N-atoms are co-deposited from separate C and N sources onto a common substrate. These methods rely in large part on endothermic insertion of energetic N-atoms into the C-C bonds that either exist in the incident C-atom beam or which freely form in the growing film. Consequently, only a small fraction of the N-atom beam contributes to growth of beta-C_3N_4 and there is a resultant adverse tradeoff between film growth rate and product quality as measured by the film N / C ratio which is typically less than the

theoretical value of 4 / 3. Presence of excess carbon in the carbon-nitrogen films is responsible for degradation of the desirable optical and mechanical properties of the nitride.

Our approach to synthesis of carbon nitride is based on a chemical rather than physical route, which involves starting with a single CN type precursor that is both more energetic and more nitrogen rich than C_3N_4, and which is driven by energy transfer to facilitate elimination of excess nitrogen as a gaseous byproduct. The NCN radical, which can be derived in situ from dissociation of parent or donor molecules such as cyanogen azide (NCN-NN), is of particular interest in this regard since it meets the above requirements and also sterically hinders formation of direct C-C bonds. For reasons of chemical purity and ease of synthesis, we also investigated cyanuric triazide (CTA) which is the aromatic ring trimer of cyanogen azide. These intermediates were prepared in the laboratory from commercially available stable reagents and dissociated either by contact with excited nitrogen molecules obtained from a continuous discharge in a low-pressure flowtube reactor or by exposure to ultraviolet radiation from a low-pressure mercury discharge lamp. The resulting films were subjected to a variety of optical, chemical, and physical diagnostics to ascertain both their crystalline structure and utility in coating applications.

Theoretical / Experimental Collaborations

The present work (for AFOSR) followed an earlier startup project that was initially supported with lab director's funds from the Materials Laboratory at Wright-Patterson AFB. This funding was administered under an existing contract at the Science Center (F33615-92-C-59678) and through a parallel sub-contract with the Anteon Corporation (F33615-92-D-5000, Delivery Order 72 / Subtask 3). The present work has also been carried out in parallel with an ongoing effort at

the Science Center by Dr. Alan Harker and his associate, Mr. Chris Linnen that is also funded directly by WPAFB under contract (F33615-96-D-5835). This collaboration effectively couples the experience and facilities of two groups at Science Center, which are specialized in azide chemistry and solid film characterization. All data from both projects has been reported equally to the project managers at both AFOSR and WPAFB. A second collaboration, at no cost to the government, involved the services of Dr. Harvey Michels at the United Technologies Research Center in E. Hartford, CT who performed ab intio calculations of NCN and cyanogen azide to supplement experimental spectroscopic data available from the scientific literature in regard to these key intermediates.

Many details regarding the present work are contained in the publication manuscripts included as part of this report. In the following sections, work covered by these publications will be reviewed at the summary level, while a full account will only be given of the results obtained beyond work already covered in the manuscripts.

SYNTHESIS OF CARBON-NITROGEN FILMS

Preparation of Donors

Cyanogen Azide

Two methods were employed to generate gaseous cyanogen azide. The first method involved reacting sodium azide with cyanogen chloride in propylene carbonate solvent. The reaction completes in 2 – 3 hours at 60 – 70°C and yields the azide gas as well as carbon dioxide (from solvent decomposition) and unreacted cyanogen chloride vapor. Separation of product gas from the low vapor pressure solvent proved to be highly effective. The gas phase products were

diluted in helium and used to grow films without further purification. The second method involved reacting a mixture of solid sodium azide and solid cyanogen bromide, in the absence of any solvent, upon warming to the melting point of the cyanide (~ 65°C) for 1 – 2 hours. This process yielded azide gas and unreacted cyanogen bromide vapor, which were similarly diluted in helium before being used to grow films. The second process was eventually preferred due to the lower cost of the bromide reagent compared to the chloride, easier loading and cleanup of the reactor, and complete elimination of oxygen impurities that stem from the carbon dioxide impurity obtained as a byproduct of the solvent-based chloride method. Attempts to separate out the bromide impurity from cyanogen azide using cold traps proved extremely difficult due to nearly identical vapor pressure curves and the explosive potential of the azide when condensed to its liquid or solid phase. In either case, presence of the azide gas was readily determined by use of an Fourier Transform infrared (FT-IR) absorption diagnostic tuned to the characteristic band at 1255 +/- 10 wave numbers.

Cyanuric Triazide

Owing to extreme difficulties in producing chemically pure cyanogen azide, we also investigated use of cyanuric triazide (CTA) which can be readily obtained in pure form. This trimer corresponds to three cyanogen azide molecules linked into an aromatic six-membered ring of alternating C and N-atoms, with azide groups attached to each of the C-atoms. Since this material is a high density solid as well as a known primary explosive, it was synthesized in small 3-gram batches for safety reasons. The following synthetic procedure was adapted from instructions obtained from Dr. Jens Franken at the University of Illinois (Urbana). Mix 5 grams of sodium azide with 20 ml of water and in a separate beaker mix 3.1 grams of cyanuric chloride with 30 ml of acetone. While stirring, add the acetone solution to the water solution slowly. Heat

the combined solutions to 40 – 50°C for 5 – 10 minutes. Cool the solution and pour into a polyethylene-baking pan secured to a mechanical rocker and allow the solvents to thoroughly evaporate (typically over night). Add 200 ml acetone and resume rocking for approximately one hour, adding additional acetone as required to compensate for evaporation (not all of the solids will dissolve). Cease rocking and allow the remaining solids to settle before decanting the clear solution into two plastic ice cube trays, equally dividing the solution (approximately) between the 32 cells. Allow the solvent to evaporate. After several hours each cell in the ice cube tray will carry approximately 100 milligrams of chemically pure CTA which appears as a thin white crystalline ring adhering to the sidewalls. Gently scrape off the triazide from the sidewalls, one cell at a time, and do not recombine the separated charges. Since there is some probability of accidentally setting off the azide charge by scraping, and since even 100 milligrams of CTA gives a very loud report, gloves, ear protection and appropriate eyewear are required as a minimum during this phase of the operation. CTA is shock sensitive and can be easily set off by impact or heat which results in a very brissant (sharp) detonation. The above preparation is suitable for small laboratory experiments and some changes in methodology will be required to scale the process for industrial application.

Several experiments were performed to evaluate the physical and chemical properties of CTA with respect to the present application. In the first experiment, 200 milligrams of CTA were dissolved in acetone and admitted to a 200-ml stainless steel bomb with an attached pressure transducer. The acetone was pumped off to vacuum before sealing the bomb and quickly lowering it into an oil bath that was heated to 100°C. From the initial fast rise in pressure we deduced an approximate CTA vapor pressure of 0.7 milliTorr at 100°C. This vapor pressure is too low for practical use in the flowtube reactor. Consequently, our next step was to investigate the feasibility of thermally dissociating CTA to yield a clean source of cyanogen azide. The

feasibility of such a thermal decomposition reaction depends on opening the ring structure of CTA at a significantly higher rate than is characteristic of azide dissociation. From our previous work with stored cyanogen azide, we determined that cyanogen azide decay becomes significant in 5 – 10 hours at 65°C. The CTA bomb temperature was therefore lowered to 65°C and the long-term rate of pressure growth was monitored over the next two days. Temporarily removing the bomb from its heated oil bath and observing concomitant pressure stabilization verified that our results were not due to slow leaks in the container. With the temperature maintained at 65°C, bomb pressure increased at a steady (linear) rate, suggesting that ring opening and azide dissociation have widely separated rate constants. Since both processes give rise to measurable pressure increase, only one of them can rate-limit the decomposition process. The measured rate of pressure increase extrapolated to complete dissociation of the CTA charge in approximately one month's time. This last result shows that thermal dissociation of CTA is not a practical route to synthesis of clean cyanogen azide, since any azides that are released due to ring opening would decay before a significant fraction of the charge was converted. This conclusion was further verified upon admitting gas from the bomb to an FT-IR absorption spectrometer which showed no traces of either cyanogen or cyanogen azide (the measured pressure rise was entirely due to nitrogen). Consequently, it was necessary to seek an alternative to the flowtube as a method to grow carbon-nitrogen films from this chemically pure donor.

A small sample of CTA was also subjected to a thermogravimeteric analysis (TGA) in which the sample weight is monitored as a function of the temperature of a surrounding air stream that increases slowly (60°C / hour). As shown in the figure below, the rate of mass loss picks up above 65°C and accelerates rapidly to completion at 130°C.

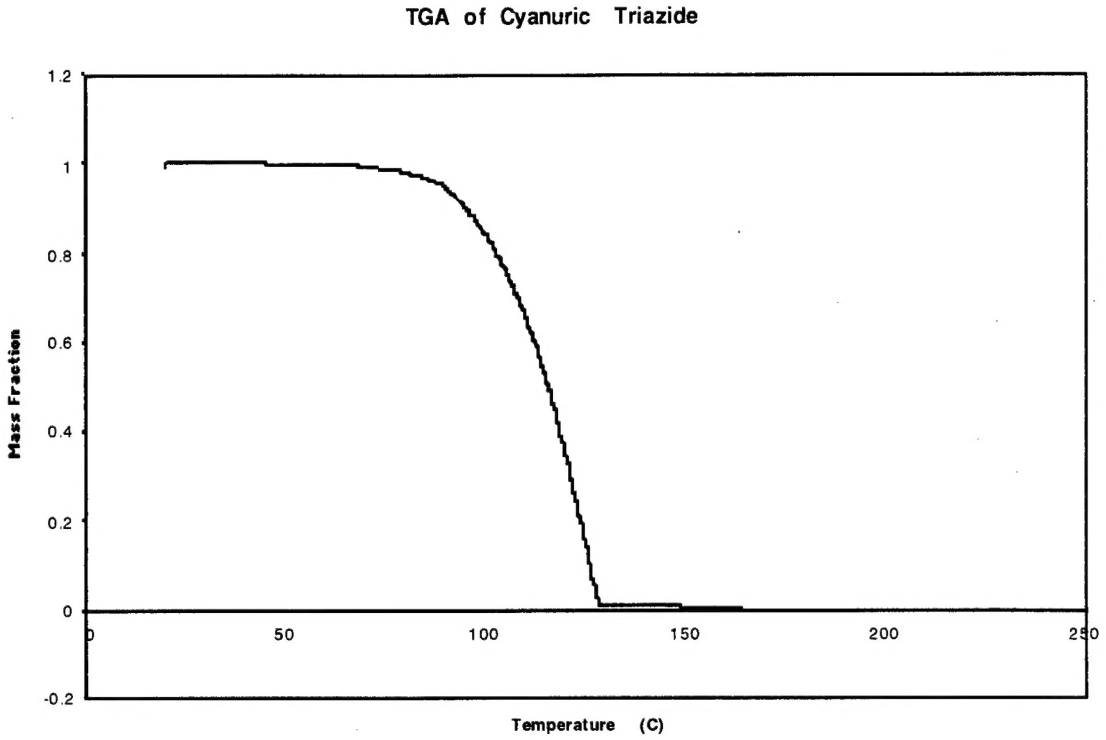

The TGA results shown above were differentiated logarithmically and plotted vs reciprocal temperature (Arrhenius format) in the figure below to determine an activation energy for decomposition of CTA. From the slope of the straight-line portion of this curve one obtains 1.04 eV as the activation energy parameter. Deviation of the Arrhenius plot from linearity at high temperature is due to an accelerating rate of CTA decomposition. This result is consistent with mass loss caused by reactive decomposition and self-heating above the temperature of the surrounding air stream. Mass loss due to thermal evaporation (self-cooling) would have produced the opposite effect. A best fit to linear data in the Arrhenius plot yields $\Delta m / m = (2.4 \times 10^6 / \text{second}) \exp(-12{,}000 / T)$ as the kinetic rate equation for fractional mass loss ($\Delta m / m$) of the solid CTA charge, where the temperature (T) is expressed in degrees K. Since the measured activation energy for CTA mass loss agrees closely with the activation energy for cyanogen azide dissociation obtained from Michels' ab initio study, it follows that decomposition of the

ring trimer is initiated by azide fracture rather than by ring opening. Additional ab initio calculations of CTA by Michels are in progress to verify this result.

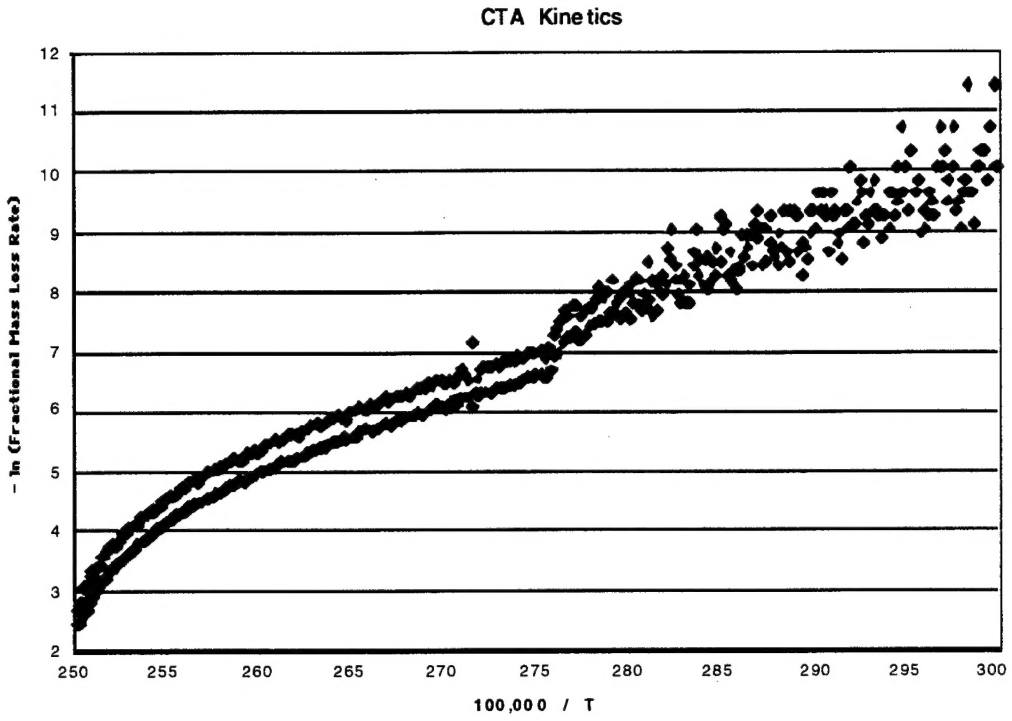

Film Deposition / Flowtube Reactor

Longitudinal Discharge

The first carbon-nitrogen films were generated by reacting cyanogen azide with discharged nitrogen in a low-pressure flowtube reactor. Passage of nitrogen gas through an upstream discharge produced long-lived vibrationally excited states that collisionally transferred energy to the azide upon mixing with the injected donor gas. Transfer of energy from discharged nitrogen to cyanogen azide ruptured the weak NCN-NN bond, thereby liberating free NCN radicals which are the growth species. The carbon-nitrogen films subsequently grew further downstream on a

substrate suspended in the reacting flow field. Initially, ZnS substrates were used at near ambient temperature, however, later work employed a variety of substrate materials and the substrate mount was equipped with an electrical resistance heater and thermocouple for deposition of films at elevated temperature. Our initial work also used a longitudinal discharge that was powered by a neon sign transformer and was located 20 – 40 cm upstream of the azide injector. Consequently, there was sufficient time in transit for fast V-V exchange reactions to relax the non-thermal (nascent) vibrational distribution of the discharged nitrogen molecules prior to contact with the azide donor. Since dissociation of the donor is best promoted by transfer from higher vibrational energy levels, the flowtube discharge section was redesigned (as described below) to significantly decrease transit time.

Transverse Discharge

The improved discharge was formed by wrapping a copper foil around the quartz flowtube immediately upstream of the azide injector. The injector was located at the tip of a grounded stainless steel tube which ran coaxially down the centerline of the reactor. A transverse (radial) discharge between the copper foil and injector tube was energized by applying a 1 KV / 50 KHz drive to the copper foil. Current and voltage measurements in this configuration indicated comparable discharge input power to the prior longitudinal arrangement that was powered by a neon sign transformer. Use of the transverse discharge, nonetheless, significantly enhanced the rate of film growth with no concurrent increase in the rate of azide donor injection. Consequently, the enhancement was due to improved efficiency of the azide dissociation reaction. Michels' ab initio calculation of the NCN-NN bond strength suggested that $v = 4$ and above in nitrogen were required for efficient dissociation by energy transfer. A vibrational analysis of nitrogen first positive band emissions from the region of azide injection, also

confirmed a significantly higher yield of nitrogen molecules at and above the critical v = 4 energy level.

Ultraviolet Curing

Small samples of CTA (nominally 25 milligrams) were placed onto a 1-inch diameter silicon substrate which rested on top of a variable temperature hotplate. The CTA samples were covered by a (Raytheon CVD) diamond wafer as shown below. The diamond wafer was used to flatten the CTA layer which otherwise tended to bead on the polished silicon surface. Heating of the sandwich to 70 – 80°C melted the triazide and produced a thin intermediate layer which could be exposed (through the diamond) to ultraviolet radiation from a 5 Watt low pressure mercury / quartz Pen-Ray lamp. This type of lamp is commonly used for spectroscopic calibrations. Dominant 254 nm resonance radiation from the mercury lamp is well matched to the characteristic azide absorption continuum at 260 +/- 20 nm. Photochemical reactions, induced by the mercury lamp, can therefore mimic energy transfer processes that occur in the flowtube reactor.

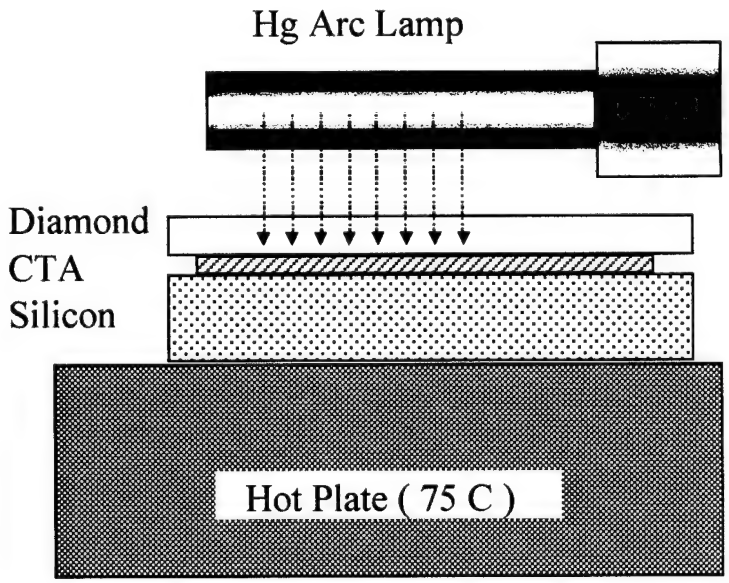

The layer of CTA (between the silicon substrate and diamond wafer) turned solid after approximately two hours of continuous exposure to ultraviolet radiation. Subsequent separation of the silicon and diamond plates fractured the film in an irregular pattern indicating strong adherence to both the diamond and silicon surfaces. Bubble formation associated with photochemical reaction byproducts (nitrogen) also degraded the quality of films obtained by this technique. An improved method involved placing the CTA charge on a silicon substrate as before and positioning the diamond wafer on top of a metal grill suspended about 1 cm above the silicon surface. Tests run in this configuration quickly revealed that film generation required both light and heat.

A very telling test was performed by removing the diamond substrate so that both ultraviolet radiation and CTA vapors (as well as any gas-phase photolysis products) could pass freely through the grill. In this case, a film grew exclusively on the upper side of the grill (facing toward the lamp). This key result clearly demonstrates that gas-phase photochemistry is insignificant and the important sequence of events was: (1) thermal evaporation of CTA, (2) gas-phase transport of vapors through the grill, (3) adsorption of CTA onto the upper surface of the grill and (4) photolysis of the adsorbed layer to generate a film. Films produced from CTA on both diamond substrates and aluminum nitride (over silicon) by the vapor transport / surface photolysis method were smooth, strongly adherent and (apart from thickness distribution over the substrates surface) visually identical to films grown in the flowtube reactor using cyanogen azide.

DIAGNOSTICS AND RESULTS

Film Thickness / Index of Refraction

Three inter-related methods were used to determine film thickness. The most accurate method involved visible reflectance spectroscopy at near normal angles of incidence. In this method, the deposited film acts as an etalon with interfering multiple internal reflections that result in an oscillating reflectance spectrum. Optical theory is used to generate a unique match between the spectral data and calculations that employ film thickness and refractive index as variable fit parameters. Additional thickness measurements were made using a surface profilometer over a step in the film produced by deposition onto a substrate that was partially masked by a removable tape. Since these independent thickness determinations were in close agreement with the corresponding interferometric results, we can have increased confidence in the refractive index measurement (n = 2.3), which is relatively close to high-grade diamond-like carbon. For films of greater depth, we obtained thickness information by comparing intensities of selected infrared absorption peaks to corresponding data obtained from thin films where the thickness was also determined by interferometry.

Electrical Conductivity

Films of 0.7 micron thickness were measured via a 4-point probe and shown to possess sheet resistivities greater than 10 Megohms / square.

Mechanical Stability / Adhesion

Both stress cracking and peeling contributed to the mechanical failure of several films. Factors which contributed to film stability included thin layers, deposition onto substrates other than silicon, deposition onto heated substrates, addition of helium diluent in the flowtube (along with

the azide donor) and use of the close coupled transverse discharge geometry. Films obtained from thermal evaporation and ultraviolet curing of CTA donor were strongly adherent and could not be removed by either scotch tape or rubbing with a standard eraser.

Thermal Stability

Films deposited onto diamond by thermal evaporation and ultraviolet curing of CTA were largely removed upon exposure to a 650°C nitrogen atmosphere for 1 hour. Subsequent microscopic examination of the substrate, however, revealed patches of a residual film of higher density. This finding suggests that our original films where composed of both hard (thermally-stable) regions of crystalline beta-phase carbon nitride as well as softer (thermally unstable) regions of polymeric paracyanogen.

Visible Absorption Spectroscopy

Films deposited onto transparent Cleartran substrates demonstrated a slightly yellow-brown coloration to the unaided eye. The visible wavelength transmission spectrum of these films showed increasing absorption at wavelengths below 550 nm, corresponding to a soft optical band gap of approximately 2.6 electron-volts.

Infrared Absorption Spectroscopy

Two broad absorption bands were observed in the infrared spectrum of films grown in the flowtube reactor, which were centered at 1600 and 3150 wave numbers. The shorter wavelength band grew rapidly upon exposure of the film to atmosphere following deposition. This absorption band is therefore thought to be caused by film oxidation or hydrolysis reactions.

Deposition of films onto substrates heated to approximately 360°C narrowed the longer wavelength infrared absorption band and stabilized the shorter wavelength band at a reduced intensity following atmospheric exposure. These results suggest that films deposited over a heated substrate are more densely packed and characterized by a reduced number of phase impurities compared to films grown at ambient temperature. Films grown at higher temperature also exhibited improved mechanical stability against cracking and peeling. This favorable result is undoubtedly due to relief from buildup of mechanical stresses caused by atmospheric reaction in the less densely packed or void regions of films deposited onto ambient temperature substrates.

The infrared transmission spectrum of a CTA generated film deposited onto a diamond substrate is shown below.

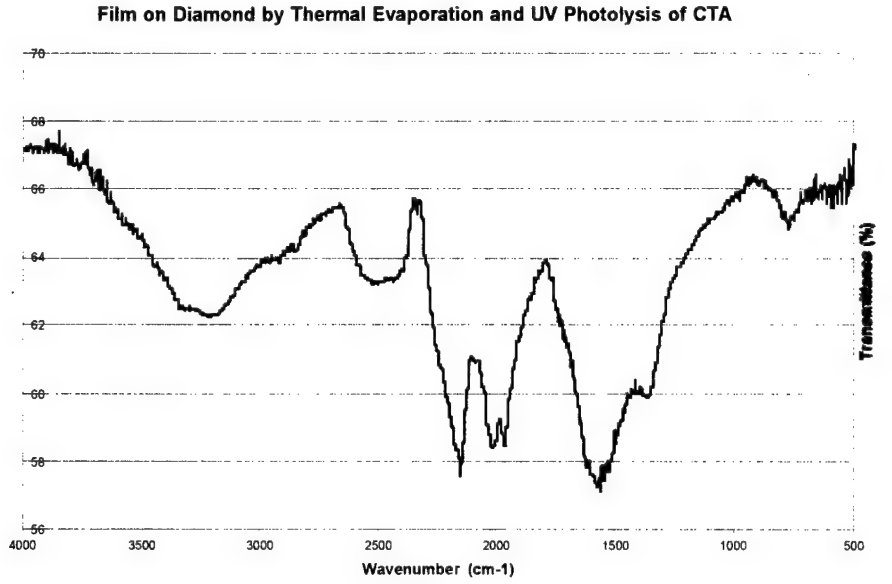

Apart from substrate absorptions (marked by vertical bars) this film exhibits the same characteristic broad absorptions at 1600 and 3150 wave numbers as seen in films grown in the flowtube reactor. Consequently, we may conclude that films grown from the chemically similar CTA and cyanogen azide donors are comparable despite the very different physical methods used in the depositions.

X-ray Photoelectron Spectroscopy

The x-ray photoelectron (XPS) spectrum of a film produced from cyanogen azide (via the chlorine based generator) included a single nitrogen peak and a split carbon peak that deconvolved into three components, corresponding to carbon bonded to carbon, carbon bonded to impurities (oxygen and chlorine) and carbon bonded to nitrogen. Comparison of the nitrogen-bonded component of the carbon peak to the unsplit nitrogen peak was consistent with the theoretically anticipated C_3N_4 stoichiometry, with approximately 40% of the total carbon in this phase and an equimolar yield in a diamond-like state.

X-ray Diffraction Spectroscopy

No discreet lines, other than from the substrate, were observed in the X-ray spectrum of any films grown at ambient temperature in the flowtube. Films deposited onto silicon carbide or aluminum nitride at about 500°C, however, revealed identical sharp diffraction lines that were not detectable in the bare substrates. Further, these diffraction lines, which appeared with good S/N ratio at lattice spacings of d = 2.703 and 1.499, agree precisely with the known strong lines of beta-phase C_3N_4. Consequently, our high temperature films have been shown to contain at least some microscopic regions of the desired hard crystalline material.

RECOMMENDATIONS

Two new routes have been established for synthesis of carbon nitride that are based on molecular dissociation of the donors cyanogen azide and cyanuric triazide (CTA). Regardless of which technology is pursued, it is clear that an effort to increase the mole fraction of hard crystalline material at the expense of softer polymers is of primary importance. While substrate temperature has been shown to have significant beneficial impact in this regard, other controlling factors need to be identified and exploited. These may include perturbations such as laser illumination and

ultrasonic agitation of the substrate or presence of additional chemical reagents in the flowtube during the process of film deposition.

The synthetic route based on photochemical dissociation of CTA, although less well developed at the present time, appears to be especially well suited to applications which demand high chemical purity as in the semiconductor industry. The electrical insulating properties and excellent adherence of this material to silicon carbide suggests its use as a gate insulator, passivation, or junction termination layer in high temperature field effect transistors and integrated circuitry. The improved substrate adhesion obtained from these chemically purer films also suggests that CTA photolysis may be the method-of-choice for optical coating applications given further development of this vapor deposition technology. The following straightforward improvements in the CTA based synthesis of carbon nitride should therefore be investigated.

1) Mount the substrate on a rotation stage to enable deposition of more uniform films.

2) Use optical baffles to prevent ultraviolet exposure of the evaporating CTA charge.

3) Use forced gas convection and ducting to carry evaporated CTA to the substrate.

4) Develop a safe method to extend the length of a coating run to enable thicker films.

Finally, regardless of the synthetic route employed, realizing the full potential of carbon nitride will require attention to optimizing bulk properties such as hardness, as well as film adhesion to substrates and uniform thickness over large areas. These areas of investigation cannot proceed independent of one another in a strictly parallel fashion because of the potential for significant

interactions, nor can they be efficiently developed in a strictly serial manner for similar reasons. Realistically, full development of carbon nitride will require the interaction of a dedicated team composed of experts in chemical kinetics and diagnostics, synthetic procedures, film technology and molecular theory.

PUBLICATIONS

The following section contains the manuscripts of two publications based on this work, the first of which has already appeared in the Journal of Physical Chemistry, Part B. The second paper is under review by the editors of Diamond and Related Materials.

Dissociation of Cyanogen Azide: An Alternative Route to Synthesis of Carbon Nitride

D. J. Benard, C. Linnen, and Alan Harker

Rockwell Science Center, Thousand Oaks, California 91358

H. H. Michels and J. B. Addison

United Technologies Research Center, East Hartford, Connecticut 06108

R. Ondercin

Air Force Wright Materials Laboratory, Wright-Patterson AFB, Ohio 45433

The Journal of Physical Chemistry B®

Reprinted from
Volume 102, Number 31, Pages 6010–6019

Dissociation of Cyanogen Azide: An Alternative Route to Synthesis of Carbon Nitride

D. J. Benard,* C. Linnen, and Alan Harker
Rockwell Science Center, Thousand Oaks, California 91358

H. H. Michels and J. B. Addison
United Technologies Research Center, East Hartford, Connecticut 06108

R. Ondercin
Air Force Wright Materials Laboratory, Wright-Patterson AFB, Ohio 45433

Received: April 14, 1998; In Final Form: June 4, 1998

Solid films composed principally of carbon and nitrogen were grown on a variety of substrates at ambient temperature in a flow-tube reactor by upstream mixing of cyanogen azide, cyanogen, or cyanogen halides with active nitrogen obtained from an electrical discharge. Ab initio calculations and dependence of deposition rates on both choice of donor and N atom production suggests that NCN radicals are a critical growth species. The films obtained are electrically insulating with a refractive index of 2.3 at visible wavelength and are optically transparent from 550 nm out to at least 14 μm with the exception of two broad absorption bands centered at 1550 and 3250 cm^{-1}, the latter band growing in upon exposure of the film to atmospheric moisture. Film analysis by X-ray photoelectron spectroscopy revealed comparable concentrations of both carbon-to-nitrogen bonds (with approximate C_3N_4 stoichiometry) and diamond-like carbon-to-carbon bonds as well as minority bonding of carbon to impurities.

Introduction

Cohen[1] intially predicted that carbon nitride (C_3N_4) could exist in a stable hexagonal phase analogous to β-Si_3N_4 with hardness greater than natural diamond, and many investigators have explored a variety of physical methods to prepare thin films of this interesting new material. Typically, small carbon clusters and energetic nitrogen ions are obtained from separate sources and co-deposited onto a common substrate in a suitable vacuum chamber. Deposition onto heated substrates has also been used to inhibit formation of softer thermally unstable paracyanogen structures as well as to promote crystallinity in the films obtained by activating the surface layer and destabilizing more weakly bound amorphous growth sites at the reactive interface.[2−5] Thermal control, however, cannot be applied to all substrate materials of interest. Finally, since every C atom in C_3N_4 is bonded exclusively to four adjacent N atoms, physical methods are characterized by endothermic insertion of N atoms into C−C bonds that either are present in the original clusters or form upon growth of the film.

Because of difficulties inherent to physical N atom insertion, we have sought a chemical synthesis in which the critical C−N bonds are established prior to film deposition. From this point of view, a precursor should contain only N and C atoms with no direct C−C bonds and full coordination of all carbon bonds to nitrogen, as well as an atomic N/C ratio greater than 4/3 and thermodynamic potential greater than C_3N_4. The NCN radical meets these criteria and is thought to be a superior growth species, since formation of the nitride from this intermediate is thermodynamically driven by elimination of gaseous nitrogen (N_2) which escapes from the growing film while steric factors simultaneously hinder creation of new C−C bonds.

Over the past decade, our laboratory has investigated dissociative reactions of the halogen azides (XN_3, X = F or Cl), which are useful for powering short-wavelength chemical lasers.[6,7] Collisional transfer of modest amounts of thermal, vibrational, or electronic energy to these parent or donor molecules results in prompt fragmentation and efficient liberation of metastable electronically excited NX* radicals. Also, once a critical threshold is achieved, the dissociation process becomes autocatalytic due to feedback of released energy from excited products to residual azides by an energy-transfer mechanism. In the case of FN_3 dissociation, feedback of released vibrational energy (v) occurs from primary byproducts ($FN_3 \rightarrow N_2(v) + NF^*$) as well as secondary products of collisional quenching ($M + NF^* \rightarrow M(v) + NF$) and self-annihilation reactions ($2NF^* \rightarrow N_2(v) + 2F$) of the metastable species.[8] Coombe and Ray[9,10] have studied analogous dissociation mechanisms in ClN_3 which liberate electronically excited metastable (NCl*) radicals, and these authors provide a similar explanation for the chained decomposition.

On the basis of commonalities in the above research data, it seemed feasible that a rich source of NCN could also be obtained from analogous dissociation of the (X = CN) pseudohalogen azide. Prior matrix isolation and photolysis studies of cyanogen azide (NCN_3) by Milligan and later by Krogh also suggested this possibility.[11,12] Rapid self-annihilation of NCN radicals via the reaction ($2NCN \rightarrow 2CN + N_2$), however, constitutes a potential difficulty in this scheme that is also implied by analogy to the known kinetics of NF* and NCl* decay following dissociation of the corresponding parent azides.[6,7]

In this work, a primary stream of helium (He) diluent and N_2 passes through an electrical discharge before mixing on-

S1089-5647(98)01847-1 CCC: $15.00
Published on Web 07/15/1998

the-fly with a secondary stream of donor NCN_3 molecules and He diluent in a low-pressure flow-tube reactor. Electronically or vibrationally excited metastable (N_2*) molecules and N atoms produced in the discharge[13-17] react with the injected donor and liberate dissociation products that grow solid films of high carbon and nitrogen content on a substrate suspended downstream in the flow. Alternate donors including cyanogen (NCCN), cyanogen chloride (ClCN), and cyanogen bromide (BrCN) were investigated in like manner. Issues germane to this coating process include the relative importance of N atoms versus N_2* molecules in reaction with the donor species, the roles of NCN vs CN as species potentially related to film growth at the substrate, and characterization of the resulting solid film product. Similar carbon−nitrogen films have only recently been deposited in our laboratory at substrate temperatures up to 375 °C. For the most part, the films described herein were formed at ambient temperature and are therefore not optimized with respect to crystallinity, adhesion, or mechanical characteristics (hardness and surface friction) that will be addressed in subsequent publications.

Theoretical Section

Covalent azides, of the XN_3 type discussed above, have relatively weak central bonds[6,7,18-22] and dissociate to form electronic ground-state N_2 and corresponding halogen or pseudohalogen nitrene (NX) fragments along the lowest available potential energy surface. Since these azides and N_2 both have singlet ground states, while halogen nitrenes have triplet ground states, XN_3 dissociates adiabatically into the first electronically excited NX(a $^1\Delta$) state which is metastable, while ground-state NX radicals correlate with excited states of the azide via a repulsive $^3A''$ potential energy surface. The excited triplet states of N_2 lie too high relative to the azide ground state to play any significant role in the dissociation process.[23,24]

A weak potential barrier on the singlet surface separates the azide ground state from its correlated NX* + N_2 products, and adiabaticity of the dissociation reaction depends critically on an intersection of this surface with the repulsive triplet state. If the crossing occurs inside the potential well, as in HN_3, then it is encountered many times due to molecular vibrations before surmounting the barrier to dissociation.[25,26] These conditions result in a loss of adiabaticity and formation of ground-state triplet NX products via a low probability per encounter tunneling mechanism. When the singlet−triplet crossing occurs on the product side of the barrier, it is encountered only once as the molecule dissociates, and consequently metastable singlet NX* products are formed with near unit quantum efficiency.

Previous theoretical and experimental investigations[6,7] have demonstrated that adiabatic dissociations of FN_3 and ClN_3 occur over reaction barriers of approximately 0.5 and 0.7 eV, respectively. In the case of FN_3, the critical singlet−triplet crossing occurs on the product side of the reaction barrier, resulting in exclusive production of NF(a $^1\Delta$), whereas in ClN_3 the crossing occurs nearer to the peak of this singlet potential energy surface, and both excited singlet and ground-state triplet NCl dissociation products are obtained.[27] Although there have been previous theoretical studies[29-31] of NCN_3, the nature of potential energy surfaces leading to dissociation products has not been investigated in detail, and there is a lack of prior gas-phase experimental results bearing on this process. Consequently, to aid the present investigation, two of the authors (Michels and Addison) have carried out an ab initio study of the lowest singlet and triplet surfaces of NCN_3 as well as a preliminary investigation of resulting NCN excited states that are formed by the dissociation reaction.

TABLE 1: Calculated Electronic States of NCN @ R(C−N) = 1.2 Å

symmetry	E (hartrees)	T_e (eV)[a]/T_e (eV)[b]
X $^3\Sigma_g^-$	−146.708 863 9	0.00/0.00
a $^1\Delta_g$	−146.685 798 1	0.63/1.42
b $^1\Sigma_g^+$	−146.684 729 9	0.66/1.45
c $^1\Sigma_u^-$	−146.588 427 2	3.28/4.07
A $^3\Sigma_u^+$	−146.585 059 2	3.37/3.37
B $^3\Delta_u$	−146.583 390 0	3.41/3.41
C $^3\Pi_u$	−146.549 873 8	4.33/4.33
d $^1\Pi_u$	−146.529 292 2	4.89/5.68
D $^3\Pi_g$	−146.517 589 5	5.21/5.21
e $^1\Pi_g$	−146.502 692 8	5.61/6.40

[a] CASSCF (10, 6)/6−311+G(d) level of theory. [b] Singlets shifted by +0.79 eV to match B3LYP/6-311+G(2df) results at the a $^1\Delta_g$ state.

Electronic States of NCN. Excluding core electrons, the molecular orbital configuration of NCN with the lowest electronic energy is $(1\pi_u)^4(4\sigma_g)^2(3\sigma_u)^2(1\pi_g)^2$[X $^3\Sigma_g$] and low-lying excited states are formed by variations of the $1\pi_g$, $3\sigma_u$, and $1\pi_u$ occupancy. To achieve balance in calculation of the ground and low-lying excited states of NCN, a full CASSCF wave function[32,33] was constructed for the $1\pi_u$, $3\sigma_u$, $1\pi_g$, and $4\sigma_g$ orbitals. The distribution of 10 valence electrons among six valence orbitals resulted in 15 triplet-state configurations and 21 singlets. Several basis sets were explored, and the Pople 6-311+G(d) triple-ζ + polarization + diffuse basis[34] was chosen as a balance between complexity and computer time.

Both the ground and low-lying excited states of NCN are known to be linear and symmetric.[35] Preliminary calculations demonstrated the NCN ground and excited states to share a common potential minimum, and a fixed N−C bond length of 1.2 Å was chosen. The calculated spectra, given in Table 1, show the lowest singlet state to have $^1\Delta_g$ symmetry analogous to NCl and NF. The (000−000) bands for the X $^3\Sigma_g^-$−C $^3\Pi_u$ and a $^1\Delta_g$−d $^1\Pi_u$ transitions of NCN are found experimentally at 3.77 and 3.73 eV, respectively.[35,36] Our calculated term values for these transitions are about 12% too large, as the CASSCF procedure does not properly account for correlation effects, which contribute most significantly to errors in the singlet−triplet energy difference. The results in Table 1 should therefore be viewed as a general guide to locating electronically excited states of NCN, and more detailed calculations using correlated wave functions are required for a precise determination. Since the intersystem term value for the X $^3\Sigma_g^-$−a $^1\Delta_g$ transition is not known experimentally, calculations for these two symmetries were also carried out at a higher level of theory.

Clifford et al.[37] recently reported ab initio results of calculations on NCN and NCN^- using correlated wave functions for both the X $^3\Sigma_g^-$ and a $^1\Delta_g$ states of NCN at three different levels of theory based on the CBS approximations.[38,39] In the order of increasing accuracy, these authors found T_{00} = 1.525, 1.286, and 1.249 eV for the CBS-4, CBS-Q, and CBS-QCI/APNO methods, respectively. The latter method is among the most accurate currently available with typical rms errors as low as 0.8 kcal/mol. Our calculations of the lowest triplet and singlet states of NCN were carried out at the B3LYP/6-311+G(2df) level of theory.[40] The density functional method of Becke (B3LYP), with an extended 6-311+G(2df) basis set, was also used successfully in previous studies[37] of NCN and NCN^-. We used the basis set previously employed by Clifford et al.[37] in their analysis of the NCN^- and $HNCN^-$ ions. At this level of theory, T_{00} = 1.42 eV was obtained for the X $^3\Sigma_g^-$−a $^1\Delta_g$ term values, indicating an accuracy close to the CBS-Q method. As a first approximation, the last column in Table 1 lists uncorrelated term energies that have been corrected upward by a

constant 0.79 eV (for singlets only) to match our correlated result at the a $^1\Delta_g$ energy level.

Thermochemistry. The heat of formation of cyanogen azide can be estimated from a calculated heat of the decomposition reaction ($NCN_3[^1A'] \rightarrow NCN[X\ ^3\Sigma_g^-] + N_2[X\ ^1\Sigma_g^+]$) since heats of formation for both the NCN radical and N_2 are known experimentally.[41] The corresponding isogyric reaction (NCN_3-$[^1A'] \rightarrow NCN[a\ ^1\Delta_g] + N_2[X\ ^1\Sigma_g^+]$) is less certain since, as discussed above, the NCN singlet−triplet term value has not been established experimentally. The first dissociation reaction (leading to $NCN[X\ ^3\Sigma_g^-]$ product) was therefore examined at both the B3LYP/6-311+G(2df) and CBS-Q levels of theory, the latter being accurate to ~1.3 kcal/mol for molecules of similar complexity. Our calculated enthalpy change for the decomposition reaction is −11.3 kcal/mol (25 °C), based on CBS-Q calculated energies. Combining this result with a known heat of formation of +108.2 kcal/mol for the NCN radical, we find for NCN_3 that ΔH_f(25 °C) = +119.5 kcal/mol. Our calculated enthalpy based on B3LYP/6-311+G(2df) energies, $\Delta H_f(NCN_3, 25\ °C)$ = +119.6 kcal/mol, is also in close agreement with the CBS-Q prediction. These results are typical of the heats of formation previously calculated[7] for FN_3 and ClN_3 and are in reasonable agreement with spectroscopic estimates by Okabe and Mele.[22]

Barrier Dynamics. Activation energy for decomposition of NCN_3 was calculated at both the CBS-Q and B3LYP levels of theory. Correcting for zero-point energy, we find transition-state barriers of 1.19 and 1.18 eV (relative to the minimum in the $^1A'$ surface for NCN_3) at the CBS-Q and B3LYP levels of theory, respectively. These calculated barrier heights are significantly larger than previously determined values for FN_3 and ClN_3, in qualitative agreement with experimental evidence[6,7,12] that NCN_3 has greater thermal stability (decay time on the order of a week at ambient temperature relative to hours or fractions thereof for ClN_3 and FN_3, respectively). On the basis of the calculated barrier height, it appears that NCN_3 can be efficiently dissociated in single collisions with vibrationally excited N_2 molecules that are either at or above the $v = 4$ energy level.[23]

The potential energy surface of ground-state NCN_3 is illustrated in Figure 1, based on optimization of all bond lengths and bond angles, at fixed NCN−N_2 separation in $^1A'$ molecular symmetry, at the B3LYP/6-311+G(2df) level of theory. The repulsive $^3A''$ surface was subsequently calculated using parameters optimized for the singlet state. Figure 1 illustrates the $^1A'$ and $^3A''$ surfaces of NCN_3 crossing near the singlet surface maximum of the dissociation barrier, similar to ClN_3. We therefore expect metastable singlet NCN(a $^1\Delta_g$) molecules to be the most favored reaction product, but some nonadiabatic branching to ground-state NCN(X $^3\Sigma_g^-$) is possible.

Production of NCN(a $^1\Delta_g$) by dissociation of NCN_3 may have a profound effect on the growth of C_3N_4 films, if these metastable species propagate in substantial yield to the substrate. The additional electronic excitation carried by such precursors can aid passage over opposing reaction barriers at the gas−solid interface, and the paired electron spin symmetry of this precursor may open other more favorable reactive channels as well.

Experimental Section

Preparation. Mixtures of NCCN, BrCN, or ClCN in He diluent gas were prepared in a stainless steel cylinder (2.5 in. i.d. × 18 in. long) using neat reagents supplied by commercial manufacturers without further purification. Mole fractions of

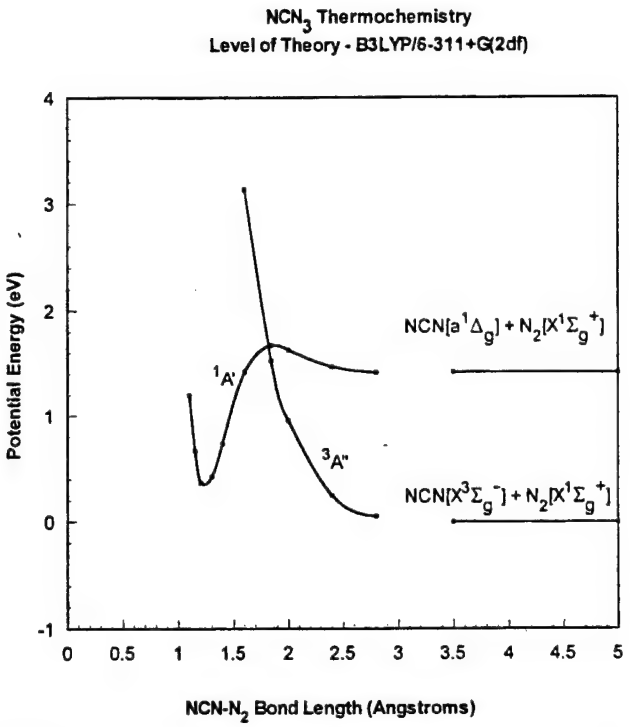

Figure 1. Singlet and triplet potential surfaces of NCN_3 relevant to molecular dissociation.

the active species were determined from pressure measurements and known vapor pressure versus temperature curves[42] of the bromide. Two methods were employed to generate batches of NCN_3 similarly diluted in He buffer gas using the same stainless steel cylinder as a reaction vessel. The first method involved adding ClCN gas to a suspension of solid sodium azide (NaN_3) in an anhydrous aprotic polar solvent.[43] Propylene carbonate ($C_4H_6O_3$) was the solvent of choice due to its desirable chemical properties and high (240 °C) boiling point[42] which facilitated both the generating reaction as well as disengagement of the gaseous azide product from solution without significant hydrocarbon contamination. In the second method, NCN_3 was generated by direct reaction of BrCN with NaN_3 in the absence of a solvent, upon heating a mixture of the solids slightly above 52 °C to melt the bromide.[42]

These reagents, and the products generated from them, are highly toxic.[44] Appropriate care must therefore be taken to avoid ingestion, inhalation, or skin exposure. Additionally, grinding of NaN_3 crystals may initiate rapid decomposition[45] into reactive sodium metal and N_2 gas, while upon condensation from the gas-phase NCN_3 forms a highly unstable explosive liquid (vapor pressure ~ 70 Torr @ 300 K).[43] Cyanogen is also a high-energy fuel capable of intense combustion with air or other oxidizing species.[44] The reagents cyanogen, cyanogen chloride, and cyanogen bromide are also highly corrosive. Tubing, valves, fittings, reactors, gauges, and storage tanks should all be constructed of stainless steel, glass, or inert polymers such as Teflon.[44] Finally, use of an oversized (300 cfm) vacuum pump with suitable discharge treatment and frequent oil changes is also warranted to prevent exposure to toxic exhaust fumes.

Approximately 12.5 g of NaN_3 was added to 120 mL of solvent in the reactor, which also contained a 2 in. long Teflon-coated magnetic stirring bar. The stainless steel cylinder, with an absolute pressure gauge attached, was then quickly pumped down to vacuum and back-filled with ClCN gas (to 1 atm pressure) with the magnetic stirrer turned off. The cylinder was

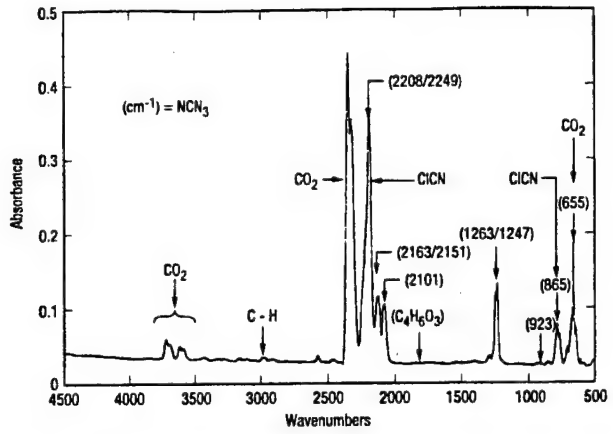

Figure 2. IR absorption spectrum of process gas stream (chloride-based NCN_3 generator).

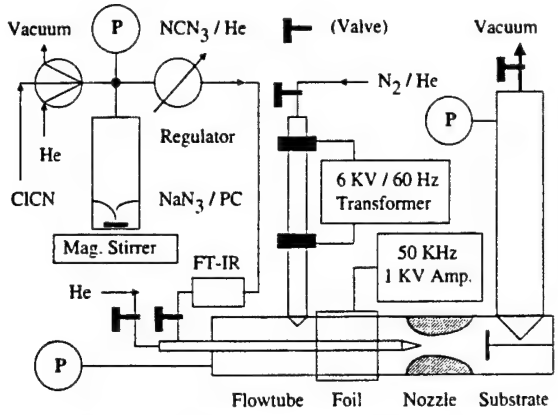

Figure 3. Schematic of the flow tube reactor used for deposition of carbon−nitrogen films.

then sealed off and stirring reactivated to absorb typically 90% of the chloride gas into the solvent in approximately 1−2 min. Subsequently, stirring was interrupted and the gas charging process repeated three more times, before finally adding He diluent to a net pressure of 80 psig. Stirring was then resumed for 2−3 h, and the lower third of the sealed-off cylinder warmed to 70 °C by means of external heating tapes. The azide diluted in He was finally withdrawn from the reservoir (still at 70 °C, with continued stirring) via a corrosion-resistant gas regulator adjusted to dispense at atmospheric pressure. This gas flow was in turn directed to a 14 cm long stainless steel FT-IR absorption cell with salt windows that evacuated to a downstream needle valve adjusted to bleed the cylinder pressure at 25 psig/h. The first hour of gas removal from the reaction cylinder was discarded to vacuum to ensure complete saturation of conductive tubing, after which the flow of dilute NCN_3 and He was redirected into the flow tube. The bromide method was carried out in the same reaction vessel using 1 g of BrCN and 2 g of NaN_3 with 80 psig of added He per batch, and reaction was complete after 2−3 h at 60 °C.

Figure 2 presents a typical FT-IR absorption spectrum of the process gas stream from the chloride-based generator. With the exception of two unresolved peaks at 444/450 cm^{-1} (not shown in these data) all of the anticipated NCN_3 bands, based on original matrix isolation work[11] by Milligan, are present at 2249/2208, 2163/2151, 2101, 1263/1247, 923, 865, and 655 cm^{-1}. Principal impurity peaks derived from carbon dioxide[46] (CO_2) at 3650, 2350, and 630 cm^{-1}, the latter band overlapping NCN_3, and residual ClCN, which also has two strong bands[47] obscuring weaker azide peaks at 2249/2208 and 865 cm^{-1}. Since the main absorption band of the $C_4H_6O_3$ solvent[46] at 1862 cm^{-1} was not detected, and there is little evidence of peaks due to hydrocarbons[46] in the vicinity of 3000 cm^{-1}, thermal separation of azide gas from the propylene carbonate solvent was highly effective. The narrow 1263/1247 cm^{-1} bands of NCN_3 are easily isolated and serve as a convenient diagnostic for monitoring the yield of gaseous azide. Typically, this absorption rises as total reservoir pressure diminishes during the course of an experiment, indicating a relatively constant partial pressure of azide gas inside the reservoir, resulting from gas equilibration with NCN_3 still dissolved in the propylene carbonate solution.

The bromide-based generator was more convenient to use and more stable in terms of azide delivery during the course of an experiment but produced somewhat lower yields of NCN_3. The CO_2 impurity previously caused by solvent decomposition was also effectively eliminated in the bromide generator which results in a cleaner FT-IR spectrum with ClCN impurity peaks replaced by comparable BrCN peaks.[47] In either case, removal of bypassed halogen cyanides from the process gas stream by use of an in-line cold trap was not practical due to lower vapor pressure of the azide,[42,43] and use of excess NaN_3 in the reactor (to consume the cyanide) unfortunately diminished the yield of NCN_3. From this last observation and the appearant stability[12] of NCN_3 in contact with dry NaN_3, one may conclude that NCN_3 has at least a deleterious slow reaction with NaN_3 that is promoted when the solid azide is dissolved either in the solvent or BrCN melt.

Flow Tube. Figure 3 is a schematic illustration of the experimental apparatus used to grow carbon−nitrogen films at ambient temperature. The flow tube was constructed of 1.375 in. i.d. quartz tubing and was operated at pressures in the range 10−15 Torr. A converging/diverging nozzle made of glass-filled Teflon (area ratio ~ 8) was positioned typically midway between the injector probe tip and a coaxially mounted 1 in. diameter substrate. The nozzle served to concentrate reactive gas flow along the centerline, thereby increasing interaction with the substrate and effectively eliminating wall losses. Assuming parabolic flow, an approximate centerline velocity of 65 m/s (upstream of the nozzle) was estimated from the cross sectional area, measured gas pressure, and a pressure versus flow curve of the vacuum system that was obtained separately by use of a calibrated electronic mass flowmeter. Pressure and velocity downstream of the nozzle depended on the position of the movable azide injector probe in relation to the nozzle throat. With the probe tip located upstream of the nozzle, upstream and downstream pressures varied less than 10%, indicating subsonic flow through the nozzle and centerline gas velocities downstream of the nozzle comparable to upstream values. Moving the 0.375 in. o.d. injector tube into or through the nozzle throat significantly restricted its open area and lead to pressure ratios as high as 3 to 1 (upstream to downstream) with corresponding acceleration of the gas to supersonic velocity at the nozzle exit plane.[48] Partial pressure of the donor species (NCN_3, NCCN, ClCN, or BrCN) in the flow tube was approximately 1 mTorr (upstream) based on total pressure measurements and mass flow rates. Rapid injection of donor molecules into the primary flow was optimized by using a conical probe tip (30° half-angle) with 12 0.035 in. diameter radial holes drilled around its circumference (normal to the reactor centerline) and by adding a variable flow of He to the secondary gas stream to allow penetration of resulting mixing jets into the surrounding stream of N_2*/He. Visually observing spatial dependence of resulting chemiluminescence demonstrated that mixing of primary and secondary flows was complete within 1 cm of the injector tip.

Discharge. Two methods were employed for production of the active nitrogen used to dissociate donor molecules. In the first method, a prepared mixture of 3−5% N_2 in He buffer gas was admitted through a 1/4 in. i.d. × 9 in. long quartz side tube, where a continuous electrical discharge was energized by a constant-current (6 kV/20 mA/60 Hz) neon sign transformer between concentric electrodes fashioned from viton O-ring sealed stainless steel tube unions. Prior to addition of azide, the above discharge filled the flow tube with an orange afterglow that is characteristic of N atom recombination.[17] Previously generated thin carbon−nitrogen films could be removed from their substrates by overnight exposure to this active nitrogen gas stream, and all substrates were cleaned in situ for several hours by this method before deposition of new films.

Substituting a more easily ionized buffer gas such as argon (Ar) for half of the He in the side tube discharge reduces both electron temperature and the yield of N atoms (in relation to N_2*) since the excited molecules have a lower excitation potential than dissociated atoms.[17] Changing buffer gas in this manner also significantly attenuates the characteristic orange chemiluminescence; however, complete substitution of Ar for He leads to discharge filamentation and less efficient volumetric interaction with the gas stream in the side tube. The three-component gas mixture was therefore used as one method to favor production of excited N_2* molecules over N atoms.

An alternate discharge generator was also employed using identical He-based gas flows as described above by wrapping a 10 cm long copper foil around the outside of the flow tube in a region upstream of the Teflon nozzle. A power amplifier applied a 50 kHz/1 kV (rms) sine wave drive to this capacitively coupled external electrode in relation to the grounded stainless steel injector tube which passed through it, and at this power level the resulting radial discharge in the flow tube produced only a faint violet-blue afterglow from the N_2/He gas stream, indicating a significantly reduced yield of N atoms. This afterglow emission, caused by $N_2(A)$ self-annihilation, was short-lived and died out over a distance of only a few centimeters in the flow.[17,49]

The discharge conditions employed in either of the generators described above are comparable to those of continuous wave carbon dioxide lasers that operate in He−N_2−CO_2 gas mixtures at similar levels of total pressure and He dilution by efficient excitation of N_2 ground-state vibrational energy levels.[50] By comparison, the corresponding excitation rates of both atoms and electronically excited states under these conditions is negligible. Measurements of both current and voltage indicated similar electrical power inputs to the two discharge generators.

Diagnostics. Visible and near-ultraviolet chemiluminescence spectra (VCS) were taken of the activated gas stream in a fixed region between the nozzle and substrate as a function of donor addition and movable injector location using a scanning (1200 line/mm) grating spectrometer at 5 nm resolution with a 1P28 or GaAs photomultiplier tube, picoammeter, and chart recorder for detection. Upon completion of a typical 2 h coating run, substrates were removed for study by visible reflectance/transmission spectroscopy (VRS/VTS), infrared transmission spectroscopy (ITS), X-ray diffraction/photoelectron spectroscopy (XRD/XPS), and scanning electron microscopy (SEM) to determine optical, chemical, and crystallographic properties.

Electrical conductivity of the films was measured by a four-point probe, and several related methods were employed to determine film thickness. For relatively thin films, which only partially covered the substrate and were dome-shaped, thickness could be estimated by counting the number of visible wavelength interference rings (rainbows) that appeared from the edge to the center. A more precise interferometric method involves measuring VRS data at near-normal incidence in the center of the film. Smooth oscillations in the VRS signal appear as a result of Etalon effect in the film with a peak-to-peak amplitude ratio dependent on film index and with periodicity dependent on both index as well as thickness according to known principles of optics[51] which have been employed in commercial instruments.[52] A two-parameter fit of the VRS data to optical theory therefore determines both index and depth of the film. In practice, it is necessary to use a somewhat more complicated model based on the same concept, which also takes into account the substrate index and reflection from its back surface to obtain the most accurate results. Some thickness results were nonetheless verified, adding certainty to our index determination, upon use of surface profilometry to measure the step height of films deposited over a removable tape mask. Comparative ITS measurements were also used to estimate depth of heavier films based on calibration of the absorption data to prior thin film results.

Results

Deposition. All tests were done with substrates mounted normal to the flow and coaxially centered in the reactor to produce near circular concentric interference rings in the finished films, as mounting of substrates inclined to the flow resulted in complicated interference patterns that were difficult to analyze for thickness. Semitransparent carbon−nitrogen films were readily grown on 1 in. diameter stainless steel, quartz, sapphire, diamond, silicon (100), silicon carbide, gallium nitride, gallium arsenide, zinc sulfide, and Cleartran substrates. Adhesion on polished silicon was poor, possibly due to surface oxidation, and these films rapidly peeled away from the substrate upon exposure to atmosphere. Attempts to remove various films on the other substrates by means of abrasion with a pink rubber eraser yielded mixed results; however, some films were obtained on stainless steel, zinc sulfide, and silicon carbide that were strongly adherent. Deposition onto silicon carbide at 230 °C improved both adhesion and stability of the film against peeling; however, this trend was found to reverse at still higher substrate temperatures. Significant differences in film depth were also obtained using a series of identical zinc sulfide substrates while holding the rate of donor injection and run time approximately constant upon varying donor type, discharge configuration, injector probe position, mixing rate, and substrate location in the flow tube.

Production of thick films was strongly favored by each of the following factors: azide donor, deposition in subsonic flow, mixing optimized for complete utilization of available N_2*, and low N atom (radial) discharge configuration. Films estimated at 4−8 μm thick were produced in nominal 2 h coating runs following the above prescription. Adjusting the He flow that was added to the donor gas stream through the mixing nozzle also had significant beneficial impact on film uniformity over the substrate surface as well as subsequent stability against peeling upon atmospheric exposure. Films obtained from ClCN were only marginally detectable, whereas comparable films grown from NCCN or BrCN were each more readily observed but still 5−10 times thinner than films grown from equimolar quantities of azide donor.

In contrast to the above observations, production of films from NCCN donor optimized using the side tube discharge with pure He diluent and film depth was significantly attenuated (in this case) if He was partially substituted by Ar to attenuate N atoms.

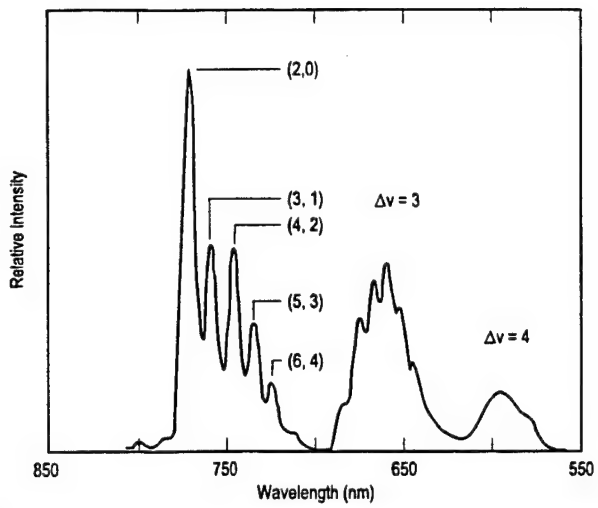

Figure 4. Visible emission spectrum of $N_2(B-A)$ afterglow produced by side tube discharge.

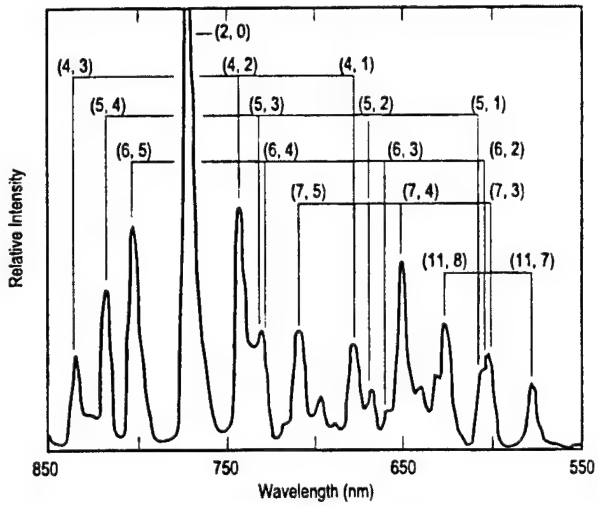

Figure 5. Visible emission spectrum of $N_2(B-A)$ afterglow produced by radial discharge.

This apparant change of direction versus the azide donor described above can be explained if NCN radicals are required for film growth as follows. Since $N_2(v)$ carries too little energy to dissociate NCCN and is present in much larger concentration than N atoms, the fast gas-phase reactions most likely to follow injection of azide donor with a weak N atom source ($N_2(v) + NCN_3 \rightarrow 2N_2 + NCN$) and addition of cyanogen donor with a more intense N atom source ($N + NCCN \rightarrow NCN + CN$) both result in production of NCN. Use of cyanogen donor in the presence of copious N atoms, however, is complicated by deleterious side reactions such as ($N + NCN \rightarrow N_2 + CN$) and ($N + CN \rightarrow N_2 + C$), the latter of which is known to occur at gas kinetic rate.[53] Consequently, potential contributions of both C atoms and CN radicals to films grown from cyanogen cannot be completely eliminated.

Spectroscopy. Partial pressure of N_2 in these experiments (~1 Torr) is high enough to ensure vibrational equilibration of the metastable A state with its ground electronic state. Consequently, changes in the vibrational distribution of ground-state N_2 are at least qualitatively reflected in the B−A chemiluminescence which derives from metastable self-annihilation.[49] Figure 4 presents an assignment of vibrational transitions emitting within the $N_2(B-A)$ band system[23] using emission data taken in the vicinity of the substrate with no donors present and side tube discharge excitation of the gas stream. In this case, an approximately quasi-thermal vibrational distribution is obtained with little relative population above $v = 6$. The vibrational temperature, however, is still large compared to ambient temperature of the gas stream, illustrating negligible loss due to slow V−T relaxation. Use of the radial discharge in place of the side tube generator produced the data that are similarly analyzed in Figure 5. Here, the vibrational distribution is significantly nonthermal, with suppression of the yield at $v = 3$ and excess relative population at both $v = 7$ and $v = 11$ in evidence. Undoubtedly, strong pumping of the N_2 vibrational energy levels occurs in either discharge generator[50] and initially produces a significant nonthermal population[54] which equilibrates in transit due to rapid V−V energy transfer. Consequently, the closer coupling and superior yield of vibrationally excited N_2 molecules (at or above the $v = 4$ energy level) associated with use of the radial discharge accounts in large part for the higher deposition rates obtained in this discharge configuration with use of the azide donor.

Reaction between discharged N_2 and NCCN donor produced essentially no observable chemiluminescence at visible wavelength in the flow tube even with suppression of the N atom afterglow, while substituting BrCN, ClCN, or NCN_3 in place of cyanogen produced pale orange, green, and yellow chemiluminescent emissions, respectively, that were each long-lived in the flow tube. Recordings of VCS in the absence of donor injection demonstrated characteristic emissions of the $N_2(B-A)$ first positive band system in the >470 nm wavelength region,[23] with a great majority of the chemiluminescence intensity beyond visual range in the near-infrared. Donor addition yielded no new emission peaks that were not also found in the discharged N_2 afterglow without donor present, with the sole exception of isolated narrow tail bands at 385 nm assigned to the CN(B−X) transition.[55] Consequently, the visually observable effects of various donors on the chemiluminescence spectrum were all caused by changing intensity distributions within the vibrational manifolds of excited $N_2(B)$ molecules.

The CN(B−X) intensity initially scaled linearly with addition of NCCN donor and eventually saturated due to depletion of N_2^*. A similar scaling relationship was obtained with use of the azide donor until the concentration of NCN_3 (as measured by absorption at 1263/1247 cm^{-1}) rose above a critical level in the region of ~10% peak attenuation, beyond which the intensity of CN(B−X) chemiluminescence increased markedly. As mentioned in the Introduction, threshold behavior for the onset of autocatalytic decomposition is anticipated from this energetic donor due to chain reactions that feed back released chemical energy to residual azide molecules.

No measurable NCN(A−X) emission[56] at 329 nm was detected, and narrow bands of NCN analogous to the well-known vertical a−X and b−X forbidden intercombination transitions[6,7,23] of NF or NCl were not observed within the range of detector sensitivity for any of the donors studied. On the basis of correlated ab initio results presented earlier, the a−X and b−X transitions of NCN are expected in the spectral vicinity of 900 nm; however, these bands are also anticipated to be very weak due to higher molecular symmetry of NCN, which adds a parity selection rule to the spin and orbital angular momentum constraints that also forbid such NX transitions in general. Since these very weak NCN transitions unfortunately fall into the same spectral region as the intense and ubiquitous N_2^* discharge afterglow, their detection is most problematical.

In contrast to the above discussion, the vicinity of allowed NCN(A−X) emission is spectroscopically clear, and intuitively one might expect that if nearly resonant CN(B−X) emission was excited, for example, by energy transfer from metastable

$N_2(A)$, then some 329 nm chemiluminescence should also be in evidence. Transferring 6.2 eV of electronic energy[23] from $N_2(A)$ results in dissociation of NCN as opposed to CN chemiluminescence, however, because the reactions (NCN → N_2 + C and NCN → CN + N) have respective thermodynamic energy thresholds[40] of 2.5 and 4.3 eV while at least 7.4 eV are required to dissociate CN. Similar considerations also apply to the known parallel $N_2(A)$ + NCN_3 → $2N_2$ + NCN(A) reaction[57] and the as likely parallel $N_2(A)$ + RCN → R + N_2 + CN(B) processes in which R = Cl, Br, or CN. These reactions are each less exothermic than the corresponding direct energy transfers described above; however, as shown in the Theoretical Section the heats of formation of NCN_3 and NCN(X) only differ by about 0.5 eV, which is insufficient to stabilize the former reaction against branching into additional dissociative product channels. The branching ratio from $N_2(A)$ into NCN(A) is therefore expected to be very small compared to similar excitations of CN(B) in either case. Consequently, the presence or lack of NCN radicals in the flow tube cannot be reliably evaluated from observations of spontaneous chemiluminescence, and more definitive methods such as laser-induced fluorescence are required instead to make this determination. Finally, while $N_2(A)$ may play a role in exciting some observable short wavelength emission, it has negligible influence on film growth. Due to limited production in the discharge and very fast self-annhilation[49] $N_2(A)$ is limited to concentrations that are small compared to the added donor.

Kinetics. Based on selection rules already discussed, radiative decay of metastable NCN(a $^1\Delta$) is expected to be as slow or slower than the analogous 0.2/s[58] and 0.7/s[7,59,60] transitions in NF and NCl, respectively. Spontaneous emission therefore contributes negligible loss of NCN* while in transit to the substrate. Consequently, the balance of metastable versus ground-state NCN radicals arriving at the film surface depends solely on collisional relaxation and reactive phenomena.

The observed strong preference for azide donor, as a source of NCN in the absence of significant N atoms, requires sufficient kinetic lifetime in active flow for these radicals to propagate to the substrate before substantial removal by self-annhilation. This condition, in turn, sets an approximate upper limit on the magnitude of a corresponding NCN self-annihilation rate constant (k). If t is taken as transit time in active flow between the injector probe and substrate, then the fraction of NCN molecules lost to self-annihilation depends on a dimensionless product term, k[NCN]t. Since this term cannot significantly exceed unity, consistent with the mechanism and observations discussed above, one then finds with $t \sim 1$ ms and [NCN] ~ [initial donor] ~ 3×10^{13}/cm^3 that $k < 3 \times 10^{-11}$ cm^3/(molecule s). For comparison, the rates of metastable self-annihilation in NF and NCl have been previously measured as approximately 3×10^{-12} and 3×10^{-11} cm^3/(molecule s), respectively.[6,7,61]

At low levels of donor injection, the initial rise of CN(B−X) chemiluminescence tracks the rate of parent molecule dissociation. The rise of CN(B) was spatially resolved by varying injector probe position in relation to a fixed observation zone, and these data were found to approximately correlate with corresponding variations of film thickness. Dissociation time constants for trace concentrations of NCN_3 and NCCN were measured as approximately 0.2 and 0.5 ms, respectively. Failure to grow films in supersonic flow may have also resulted due to formation of a bow shock[48] over the substrate; however, based on the above dissociation rates, transit times were too small in any case to permit efficient use of either donor under these conditions.

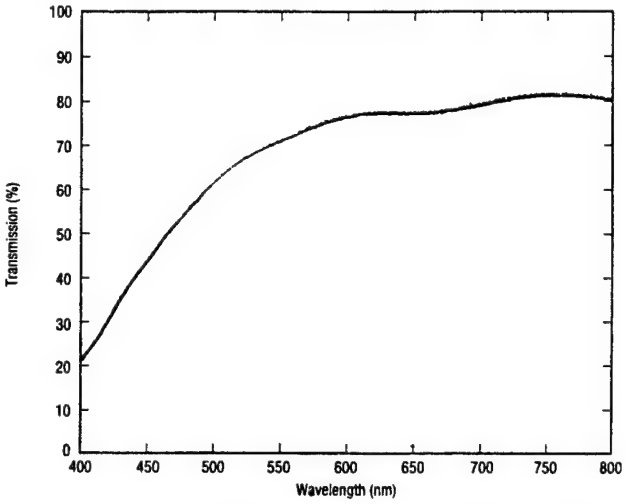

Figure 6. Visible transmission spectrum of C/N film deposited on Cleartran substrate.

Once the dissociation reaction is complete, collisional energy transfer processes are expected to support a state of local thermodynamic equilibrium in which all excited species decay at a common rate on longer time scales. The N_2* decay following injection of NCCN was monitored at fixed residence time in the flow ($T \sim 1.5$ ms) by detecting the relative intensities of CN(B−X) emission as a function of initial donor concentration [D]. Fitting this emission data to the form [CN(B)]/[D] = $A \exp - (K[D]T)$, where A is an arbitrary constant, yields an effective N_2* quench rate of $K \sim 6 \times 10^{-12}$ cm^3/(molecule s). Based on this result and typical flow tube conditions (T = 1 ms and [D] = 3×10^{13}/cm^3 for coating at 2−4 μm/h), the product K[D]T representing fractional loss of N_2* currently has a value of ~20%. Lower rates of film growth associated with use of NCCN donor in the present reactor setup could therefore be partially compensated by a 5-fold increase of the donor mole fraction before completely depleting the N_2* bath. Equivalent concentration scaling of NCN_3, however, should lead to growth rates as high as 10−20 μm/h or higher, as in this regime autocatalytic dissociation of the energetic donor enhances N_2* faster than it is depleted.

Optical. On transparent substrates, the deposited films had a faint yellow-brown coloration. As shown in Figure 6, VTS data revealed a soft band edge that is characteristic of thin films with an onset of visible wavelength absorption at 550 nm, corresponding to an approximately 2.6 eV optical band gap. The refractive index at visible wavelength and the depth of a relatively thin film deposited onto a zinc sulfide substrate were determined from VRS data shown in Figure 7 to be 2.3 and 0.8 μm, respectively, by fitting the 7° off-normal reflectance spectrum to a computer model based on the theory of dielectric layers, which also included effects of backside reflection from the substrate. The computer model was exercised using both index and thickness of the film as independent fit parameters to match period, phase, and amplitude of spectral oscillations in the reflectance data caused by film interferences. Secondary solutions were also obtained using an additional third fit parameter which uniformly scaled the known substrate index across the visible (400−800 nm) wavelength range. A satisfactory (unique) solution was indicated when both the three-parameter fit optimized with a substrate index scaling factor close to unity and similar values were obtained for the film index and thickness as in the original two-parameter solution. Subsequent profilometry measurements, given as Figure 8, also yielded a film depth of ~0.8 μm, in good agreement with our

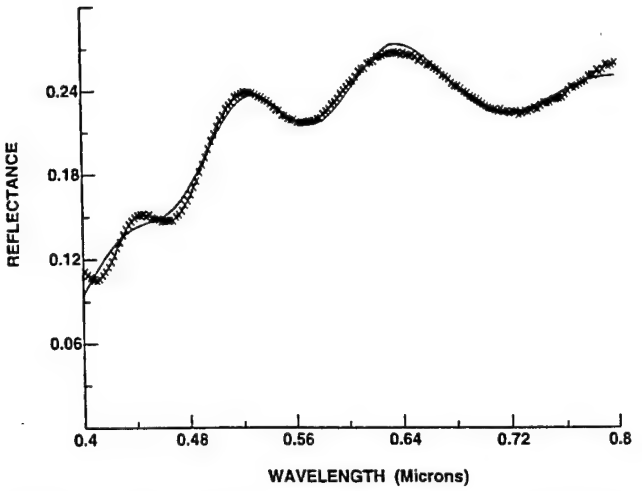

Figure 7. Visible reflectance spectrum of C/N film on ZnS substrate (×××) fit to computer model (—) used for determination of refractive index and film depth.

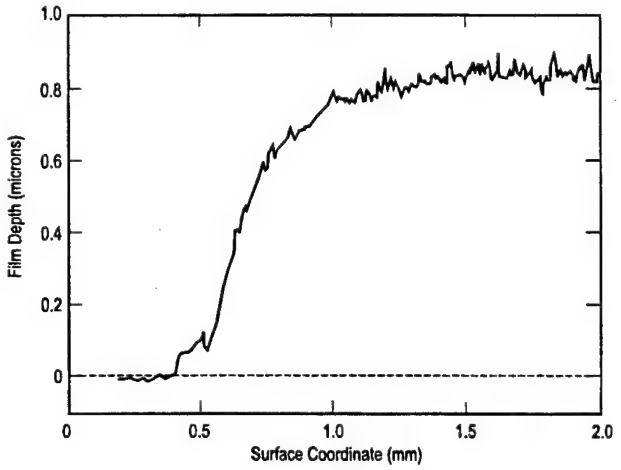

Figure 8. Film depth by surface step profilometry (C/N film deposited over a tape mask).

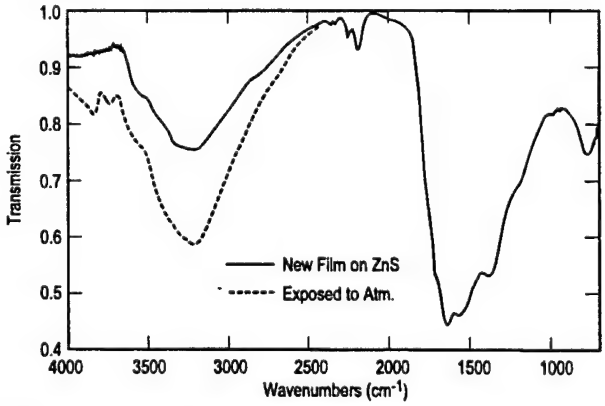

Figure 9. IR transmission spectrum of ~8 μm thick C/N film (corrected for substrate).

interferometric result. The measured 2.3 refractive index of these films is comparable to high-grade diamond-like carbon.[62,63]

Infrared transmission spectroscopy of the films demonstrated two broad and featureless absorption bands centered at 1550 and 3250 cm^{-1}, as shown in Figure 9. The ITS data presented here were generated from a thick film deposited onto zinc sulfide, and the measurement was referenced to and corrected for transmission characteristics of an identical bare substrate. The newly deposited film was maintained in a dry nitrogen

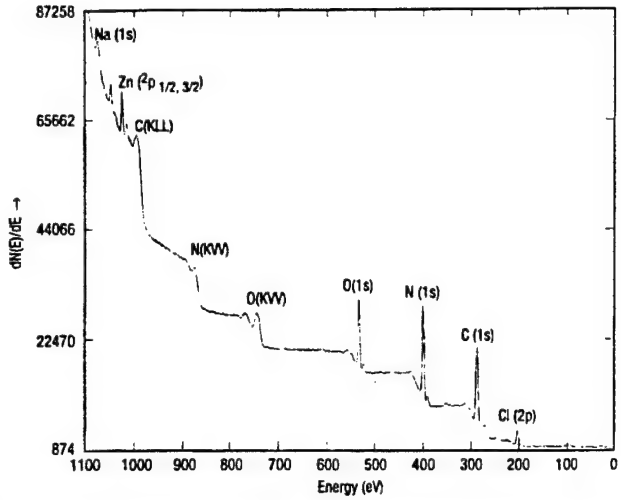

Figure 10. Low-resolution XPS scan of film grown from azide donor and process impurities.

atmosphere until placed in the spectrometer, after which repeated scans demonstrated that progressive reaction of the film with atmospheric moisture contributed to growth of the shorter wavelenth hydride stretch band. The longer wavelength bands, assignable to C−C and C−N stretching, are similar to those seen in carbon nitride films produced by co-deposition from separate nitrogen and carbon sources.[64]

Apart from differences in overall intensity of the bands due to variances in film depth, comparable ITS signatures were also obtained using samples produced from cyanogen that were relatively free of significant impurities, as the only other materials used in depositing these thinner films were He and N_2. Therefore, incorporation of impurities related to NCN_3 such as chlorine, bromine, or oxygen do not appear to significantly alter IR absorptions present in the heavier films made using azide chemistry. The extent to which such impurities may have contributed to reaction with atmospheric moisture, and indirectly to either film peeling or growth of absorptions caused by formation of air reaction products, still remains to be determined.

Chemical. A low-resolution XPS scan of a film produced from azide donor, obtained via the chloride-based generator, is given as Figure 10. These data show the film to be composed principally of carbon and nitrogen, but also significant amounts of impurity oxygen (15%) and chlorine (7%) as well as trace concentrations (<1%) of zinc and sodium. Undoubtedly, incorporation of substantially large amounts of chlorine into the film derives principally from the presence of unreacted ClCN in the flow tube as monitored by the FT-IR diagnostic. The oxygen impurity may derive either from a similar CO_2 impurity that is related to solvent breakdown in the (chloride-based) azide generator or from surface reaction of the film upon exposure to atmospheric moisture.

The overall N/C ratio of 0.53 obtained from XPS data indicates the presence of excess carbon that is either bonded to other carbon or impurity atoms in the film. Higher resolution XPS data show all the N atoms to be in equivalent sites, but the carbon line is split and deconvolves, as shown in Figure 11, to a triad of components that can be assigned to C atoms that are bonded to either other C atoms, N atoms, or impurities such as O or Cl atoms. The small central peak is easily identified with impurity sites, while comparison of the peak centered at 285 eV to similar studies of diamond-like carbon shows this signal to be caused by C−C bonding.[65] The remaining carbon peak at 288 eV is therefore assignable to C−N bonds.[66] Area analysis of the deconvoluted peaks shows that

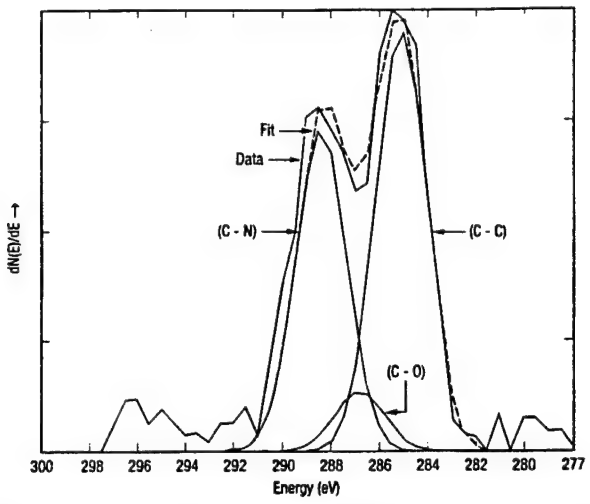

Figure 11. Deconvolution of 288 eV XPS data into single lines corresponding to C atoms that are bonded to other C atoms, N atoms or impurities.

roughly 40% of the C atoms are bonded to N atoms and the N/C ratio for this carbon component is approximately 1.3, relatively close to the anticipated (4/3) stoichiometry. Consequently, the films can be approximately characterized as near-equal mixtures of diamond-like carbon and stoichiometric C_3N_4 with lesser impurities bonded to carbon depending on the specific method of preparation. A similar analysis of oxygen-free films obtained from azide donor via the bromide generator demonstrated a single N atom line as before, no change in C−C bond density, and a corresponding increase of C−N bonding, suggesting that incorporated oxygen substitutes for nitrogen in these films.

Physical. The films obtained were electrically insulating (>10 MΩ/square @ 0.7 μm thickness). No observable discrete peaks, other than from the substrate, were seen in XRD measurements of films produced at ambient temperature. Long-range crystallographic order is therefore not present in these cases, and the films are best characterized as amorphous. Examination of the films by SEM, however, demonstrated microscopic cracking along straight lines with cracks generally meeting at right angles and individual plates curled up away from the substrate, as shown in Figure 12. These qualitative observations respectively suggest films composed of a relatively hard material with latent (short-range) crystal order that is initially formed in tension on the substrate.

More recent X-ray measurements performed on films grown on either silicon carbide or gallium nitride at deposition temperatures near 375 °C have each revealed sharp diffraction peaks at lattice spacings of 1.498 and 2.703 Å that are not present from the associated bare substrates. These data were obtained with good signal-to-noise ratio and precisely correspond to the two strongest [301] and [200] reflections of β-phase C_3N_4 previously observed by Johnson.[67] Purely crystalline films have not yet been established by intensity of the peaks observed, and it is possible that isolated microscopic crystalline domains (in an otherwise amorphous matrix) account for these results. Correlated with this finding, however, we also found that growth of the short wavelength IR absorption band due to hydride formation was also significantly attenuated in films deposited at higher substrate temperature,[64] suggesting that a more densified film structure was obtained in these cases. Details regarding these most recent findings will be included in subsequent publications.

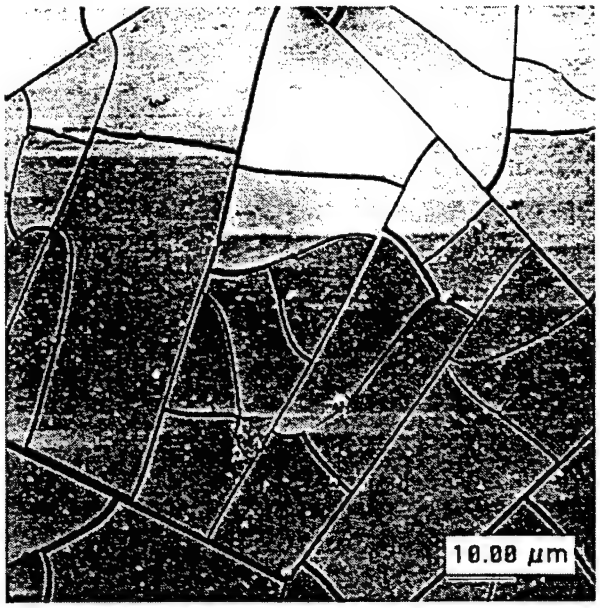

Figure 12. Scanning electron micrograph of stress-cracked C/N film on diamond substrate.

Because individual film plates do not lie flat on the substrate, it is not possible at present to perform reliable nanoindentation measurements for quantitative determination of the bulk modulus. More work is therefore required to improve film adhesion to the substrate and eliminate stress cracking before such definitive hardness measurements can be attempted. Improvements in crystallinity are also indicated in order to achieve full theoretical hardness.

Conclusions

The N/C ratio of films produced from NCN_3 is comparable to other methods previously reported.[64] Advantages of the method are relatively high growth rates in simple apparatus and ease of scalability to large volume production. Evidence of NCN as a key intermediate in the process remains inferential, and laser-induced flourescence or sensitive absorption measurements of this and other related species are required to tie down a detailed understanding of the gas-phase kinetics. Based on results of ab initio calculations, a substantial yield of singlet metastable NCN radicals is obtained from dissociation of the azide donor. The azide dissociation reaction is driven primarily by collisional energy transfer from vibrationally excited N_2 molecules at or above the $v = 4$ energy level, and it is anticipated that a significant fraction of the resulting electronically excited NCN radicals reach the substrate where differences in spin symmetry or internal energy can play a significant role with respect to film growth. The relative importance of ground versus excited states of NCN as potential growth species, however, still needs to be evaluated experimentally. Results obtained to date also illustrate a highly reactive growth surface capable of incorporating impurities related to the presence of bypassed ClCN and possibly byproduct CO_2 in the flow tube. Consequently, to the extent that CN radicals are produced in the reactor by NCN self-annihilation, excess carbon is likely to accumulate in the resulting film because the unity N/C ratio of this growth species is below the preferred C_3N_4 stoichiometry, and this condition necessarily results in formation of nonvolatile byproducts. Simultaneous optimization of both film growth rate and N/C ratio therefore requires setting the residence time in the active flow as well as donor concentration consistent with the dissociation time constant and kinetic rate coefficient of

NCN self-annihilation. Surface preparation and substrate temperature during deposition were not treated as significant variables in this initial study, and work is in progress to optimize film adhesion as well as crystallinity. Finally, related physical properties such as surface friction and hardness will in time require a detailed mechanical characterization.

Acknowledgment. The authors are indebted to their colleagues Les Warren, Randy Hall, Bill Southwell, Ellen Boehmer, Dave Marshall, Dave Deitrich, and Gary Pollack, who provided many useful discussions on synthetic chemistry as well as assistance with a variety of film diagnostic methods. This work was supported by contracts with Anteon Corporation, the Air Force Wright Laboratory Materials Directorate, and the Air Force Office of Scientific Research.

References and Notes

(1) Cohen, M. L. *Phys. Rev.* **1985**, *B12*, 7988.
(2) Ogata, K.; Chubaci, J. F. D.; Fujimoto, F. *J. Appl. Phys.* **1994**, *76*, 3791.
(3) Bousetta, A.; Lu, M.; Bensaoula, A.; Schultz, A. *Appl. Phys. Lett.* **1994**, *65*, 696.
(4) Axen, N.; Botton, G. A.; Somekh, R. E.; Hutchings, I. M. *Diamond Relat. Mater.* **1996**, *5*, 163.
(5) Ren, Z. M.; Du, Y. C.; Ying, Z. F.; Qui, Y. X.; Xiong, X. X.; Wu, J. D.; Li, F. M. *Appl. Phys. Lett.* **1994**, *65*, 1361.
(6) Benard, D. J.; Winker, B. K.; Seder, T. A.; Cohn, R. H. *J. Phys. Chem.* **1989**, *93*, 4790.
(7) Benard, D. J.; Chowdhury, M. A.; Winker, B. K.; Seder, T. A.; Michels, H. H. *J. Phys. Chem.* **1990**, *94*, 7507.
(8) Benard, D. J. *J. Appl. Phys.* **1993**, *74*, 2900.
(9) Ray, A. J.; Coombe, R. D. *J. Phys. Chem.* **1994**, *98*, 8940.
(10) Ray, A. J.; Coombe, R. D. *J. Phys. Chem.* **1995**, *99*, 7849.
(11) Milligan, D. E.; Jacox, M. E.; Bass, A. M. *J. Chem. Phys.* **1965**, *43*, 3149.
(12) Krogh, O. D.; Ward, C. H.; Hollenbeck, J. M. *J. Phys. Chem.* **1982**, *86*, 2892.
(13) Stedman, D. H.; Setser, D. W. *J. Chem. Phys.* **1970**, *52*, 3597.
(14) Setser, D. W.; Stedman, D. H.; Coxon, J. A.; *J. Phys. Chem.* **1970**, *53*, 1004.
(15) Balamuta, J.; Golde, M. F. *J. Chem. Phys.* **1982**, *76*, 2431.
(16) Golde, M. F.; Moyle, A. M. *Chem. Phys. Lett.* **1985**, *117*, 375.
(17) Boehmer, E.; Ph.D. Dissertation, Max Planck Institute Fur Stromungsforschung, Gottingen, 1990, ISSN 0436-1199.
(18) Patel, D.; Pritt, A. T.; Benard, D. J. *J. Phys. Chem.* **1986**, *90*, 1931.
(19) Christen, D.; Mack, H. G.; Schatte, G.; Willner, H. *J. Am. Chem. Soc.* **1988**, *110*, 707.
(20) Coombe, R. D.; Patel, D.; Pritt, A. T.; Wodarczyk, F. J. *J. Chem. Phys.* **1981**, *75*, 2177.
(21) Kroto, H. W. *J. Chem. Phys.* **1966**, *44*, 831.
(22) Okabe, H.; Mele, A. *J. Chem. Phys.* **1969**, *51*, 2100.
(23) Rosen, B. *Selected Constants Relative to Diatomic Molecules*; Pergammon; New York, 1970.
(24) Herzberg, G. *Electronic Spectra of Polyatomic Molecules*; Van Nostrand: New York, 1966.
(25) Schmidt, M. W.; Gordon, M. S.; Dupuis, M. *J. Am. Chem. Soc.* **1985**, *107*, 2585.
(26) Kajimoto, O.; Yamamoto, T.; Fueno, T. *J. Phys. Chem.* **1979**, *83*, 429.
(27) Benard, D. J.; Winker, B. K.; Chowdhury, M. A.; Seder, T. A.; Michels, H. H. *Proc. Int. Conf. Lasers−1991*; STS Press: 1992.
(28) Murgich, J.; Aray, Y. *J. Chem. Phys.* **1987**, *87*, 3580.
(29) Tsuda, M.; Oikawa, S.; Nagayama, K. *Photogr. Sci. Eng.* **1983**, *27*, 118.
(30) Eisenstein, M.; Hirshfeld, F. L. *Chem. Phys.* **1979**, *38*, 1.
(31) Bak, B.; Jansen, P.; Stafast, H. *Chem. Phys. Lett.* **1975**, *35*, 247.
(32) Hegarty, D.; Robb, M. A. *Mol. Phys.* **1979**, *38*, 1795.
(33) Schlegel, H. B.; Robb, M. A. *Chem. Phys. Lett.* **1982**, *93*, 43.
(34) Krishnan, R.; Binkley, J. S.; Seeger, R.; Pople, J. A. *J. Chem. Phys.* **1980**, *72*, 650.
(35) Herzberg, G.; Travis, D. N. *Can. J. Phys.* **1964**, *42*, 1658.
(36) Kroto, H. W.; Morgan, T. F.; Sheena, H. H. *Trans. Faraday Soc.* **1970**, *66*, 2237.
(37) Clifford, E. P.; Wenthold, P. G.; Lineberger, W. C.; Petersson, G. A.; Ellison, G. B. *J. Phys. Chem.* **1997**, *101*, 4338.
(38) Montgomery, J. A.; Ochterski, J. W.; Petersson, G. A. *J. Chem. Phys.* **1994**, *101*, 5900.
(39) Ochterski, J. W.; Petersson, G. A.; Montgomery, J. A. *J. Chem. Phys.* **1996**, *104*, 2598.
(40) Becke, A. D. *J. Chem. Phys.* **1993**, *98*, 5648.
(41) Chase, M. W.; et al. *JANAF Thermochemical Tables, 3rd ed.*; *J. Phys. Chem. Ref. Data* **1985**, *14*, Suppl. 1.
(42) Weast, R. C. *Handbook of Physics and Chemistry*, 60th ed.; CRC Press: Boca Raton, FL.
(43) Marsh, F. D.; Hermes, M. E. *J. Am. Chem. Soc.* **1964**, *86*, 4506.
(44) Lewis, R. J. *Dangerous Properties of Industrial Materials*, 9th ed.; Van Nostrand: New York.
(45) Material Safety Data Sheet (Sodium Azide, Sigma Chemical).
(46) Pouchert, C. J. *Aldrich Library of FT-IR Spectra*; Aldrich Chemical: Milwaukee, WI, Vol. 3.
(47) Freitag, W. O.; Nixon, E. R. *J. Chem. Phys.* **1965**, *24*, 109.
(48) Liepman, H. W.; Roshko, A. *Elements of Gas Dynamics*; Wiley: New York, 1957.
(49) Clark, W. G.; Setser, D. W. *J. Phys. Chem.* **1980**, *84*, 2225.
(50) Nighan, W. L.; Bennett, J. H. *Appl. Phys. Lett.* **1969**, *14*, 240.
(51) Born, M.; Wolf, E. *Principles of Optics*, 5th ed.; Pergammon: New York.
(52) Filmetrics, Model F20 (www.filmetrics.com).
(53) Whyte, A. R.; Phillips, L. F. *Chem. Phys. Lett.* **1983**, *98*, 590.
(54) Trainor, C. E.; Rich, J. W.; Rehm, R. G. *J. Chem. Phys.* **1968**, *48*, 1798.
(55) Tatematsu, S.; Kuchitsu, K. *Bull. Chem. Soc. Jpn.* **1977**, *50*, 2896.
(56) Beaton, S. A.; Ito, Y.; Brown, J. M. *J. Mol. Spectrosc.* **1996**, *178*, 99.
(57) Meyer, J. A.; Klosterboer, D. H.; Setser, D. W. *J. Chem. Phys.* **1971**, *55*, 2084.
(58) Malins, R. J.; Setser, D. W. *J. Phys. Chem.* **1981**, *85*, 1342.
(59) Becker, A. C.; Schurath, U. *Chem. Phys. Lett.* **1989**, *160*, 586.
(60) Yarkony, D. R. *J. Chem. Phys.* **1987**, *86*, 1642.
(61) Quinones, E.; Habdas, J.; Setser, D. W. *J. Phys. Chem.* **1987**, *91*, 5155.
(62) Moravec, T. J.; Orec, T. W. *J. Vac. Sci. Technol.* **1981**, *18*, 226.
(63) Bendow, B., Ed. *Proceedings of the DARPA Workshop on Diamond-Like Carbon Coatings*; Albuquerque, April 1992; Contract MDA 903-81-C-0151.
(64) Hu, J.; Yang, P.; Lieber, C. M. *Phys. Rev.* **1998**, *B57*, R3185.
(65) Belton, D. N.; Harris, S. J.; Schmeig, S. J.; Weiner, A. M.; Perry, T. A. *Appl. Phys. Lett.* **1989**, *54*, 416.
(66) He, Z.; Carter, G.; Colligon, J. S. *Thin Solid Films* **1996**, *283*, 90.
(67) Johnson, D. J.; Chen, Y.; He, Y.; Prince, R. H. *Diamond Relat. Mater.* **1997**, *6*, 1799.

Diamond & Related Materials

Deposition of Crystalline ß-C_3N_4 Using the Novel Precursor NCN_3

C. J. Linnen*, D. J. Benard, A. Harker

Rockwell Science Center

P.O. Box 1085

Thousand Oaks , CA 91358

cjlinnen@rsc.rockwell.com

Abstract

Carbon nitride was deposited onto SiC and AlN substrates at 360 °C using precursor NCN_3 to yield intermediate NCN radicals in a discharge initiated reactive flow deposition process. The resulting films were analyzed by X-ray diffraction as well as infrared transmission measurements. Crystalline ß-C_3N_4, with preferred 200 and 301 phase orientations, appears to be a primary growth species.

Keywords: Carbon Nitride, Thin Film deposition, X-ray Diffraction, Crystalline

Introduction

Using a wide variety of film deposition techniques, researchers have attempted to synthesize the theoretical, "super-hard" beta phase of carbon nitride (ß-C_3N_4) predicted originally by Cohen and Liu[1] (and later refined by Teter and Hemley[2] to include multiple hard phases). While some successes have been reported,[3,4,5,6] few of the approaches have actually resulted in deposition of crystalline material as verified by x-ray, neutron or electron diffraction. Many of the approaches, however, have resulted in high quality amorphous CN_x thin films, and valuable research has been done to characterize these products.[7] Lieber et al.[8] recently suggested that magnetron sputtering faces a general limitation to crystalline C_3N_4 growth imposed by decreased nitrogen content of films deposited at temperatures high enough to facilitate adequate surface mobility. Bulk growth of polycrystalline ß-C_3N_4 by RF magnetron sputtering has nonetheless been recently reported.[5]

Johnson et al.[6] have also reported deposition of large micro-crystallites of ß phase C_3N_4, as well as Teter and Hemley's alpha phase, in a matrix of amorphous CN_x using hot-filament chemical vapor deposition (HFCVD) and plasma assisted laser ablation. The diffraction peaks resulting from these films were shifted from theoretical values by tenths of degrees (2 theta < 1.5%). The exact nature of this shift is uncertain, but incorporation of Si (or other heavy atom dopants) into the films by diffusion from the substrate may be responsible.[9] The IV/V atomic valence combination in C_3N_4 provides an awkward environment for symmetry and bonding. The lone pair on nitrogen increases electron

density within the structure, causing repulsive strain in the lattice while the absence of vacant, low energy orbitals in both carbon and nitrogen precludes stabilization by orbital donation. Consequently, Si impurities are believed to stabilize the CN skeleton through donation of unoccupied orbitals to the electron rich lattice as is the case in Si_3N_4.

A chemical, rather than physical, vapor deposition approach has been taken in this study by using an energetic, nitrogen-rich precursor (NCN) that is chemically predisposed to carbon nitride formation. Although carbon bonding in this growth species is sp hybridized (as opposed to the sp^3 skeleton predicted for ß-C_3N_4), all carbon bonds are coordinated to nitrogen. This factor reduces the potential for introduction of C-C bonded phase impurities into the film and facilitates high N/C ratios.

Our previous work investigated both generation of NCN radicals from parent NCN_3 molecules, dissociated by contact with N_2 ($v > 4$), as well as growth of amorphous CN_x films on ambient temperature substrates. This paper presents the results of more recent efforts involving new growths at high substrate temperature, in which crystalline films that show strong x-ray diffraction peaks similar to those reported by Johnson et al. were obtained.

Experimental

A detailed description of the flowtube apparatus has been given in our prior publication.[10] Briefly, NCN_3 was produced by reaction of a BrCN melt with solid NaN_3

at 60°C. The azide gas was diluted in He and subsequently reacted by injection into a stream of vibrationally excited N_2 obtained from an upstream coaxial discharge designed to produce a negligible yield of atoms. Interaction of the excited nitrogen and azide-bearing streams produced intermediate NCN radicals, which subsequently coated onto substrates mounted downstream of the injector. Transit time from injector to substrate was roughly 1 millisecond at 60 m/s flow velocity. Total pressure in the flowtube reactor was 10-20 Torr and the partial pressure of injected azides was about 1 milliTorr. For this study, the apparatus was modified by addition of a heated substrate mount consisting of a 1-inch diameter round copper block welded onto a vacuum flange. A high-wattage cartridge heater powered by a variable transformer was used to heat the mount from the backside, and a thermocouple embedded into the block was used for temperature measurement.

Results

Figure 1 shows IR transmission spectra of two films grown on a SiC on Si substrate at temperatures of roughly 50°C (plasma temperature) and 360 °C. The sharp peaks at 1120 cm^{-1}, 790 cm^{-1} and 620 cm^{-1} are due to the SiC underlayer. Broad absorption in the region between 1200 cm^{-1} to 1800 cm^{-1} is due to a number of stretching vibrations including C-N and C-C single bond frequencies.[11] In the low temperature sample, these bands appear broad and convoluted compared to the high temperature sample in which the same peaks are both sharper and more structured. Since the breadth

of this band is reflective of the variety of bonding states and orientations in the film, these results suggest greater bonding uniformity in the high temperature growths.

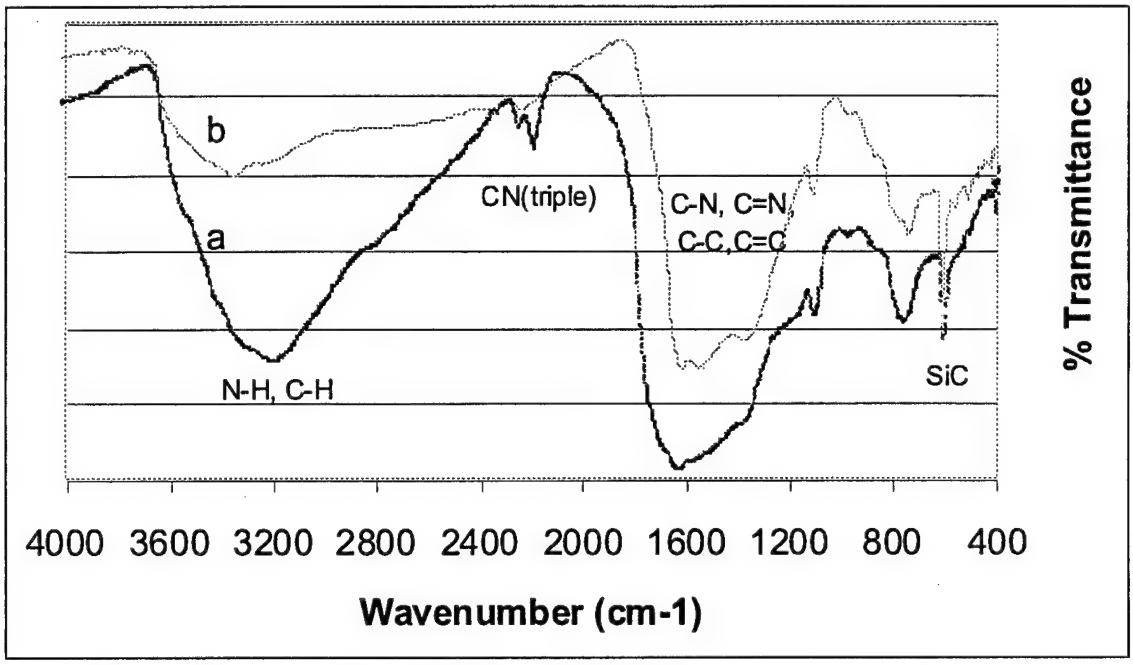

Figure 1. IR spectra of (a) film prepared at 50 C, and (b) film prepared at 360 C.

A second spectral region of interest lies between 2000 cm^{-1} and 2300 cm^{-1} where two peaks attributable to C≡N stretching exist. Because there should be no triple-bonded CN present in ß-C_3N_4, these peaks serve as a direct measure of phase impurity in the film. Comparison of the two films shows almost complete attenuation of the C≡N phase impurity in the high temperature growth sample.

The large, broad absorbance between 2400 cm^{-1} and 3800 cm^{-1} is attributable to NH or CH stretching frequencies introduced by oxidation upon exposure to atmospheric moisture. This assertion was previously verified by observing growth of the hydride peak with time under ambient conditions.[10] The degree of such oxidation is a function of film density and porosity. Since our high temperature films show a much lower amplitude absorption in this region it is reasonable to conclude that high temperature films are packed more tightly than those grown at low temperature and, hence, less subject to atmospheric oxidation.

Figure 2 shows x-ray diffraction patterns from three samples which have been vertically offset for the sake of clarity. The lower trace is the diffraction pattern of a grain oriented AlN film on a Si substrate showing AlN peaks at 2 theta = 36, 50 and 67 degrees as well as the [100] Si peak at 69 degrees. The upper trace is the diffraction pattern of a crystalline carbon nitride film grown on the same substrate at elevated temperature (no diffraction peaks were observed from films grown on unheated substrates). Sharp peaks that do not exist in the substrate can clearly be seen at plane spacings of d = 2.703 and 1.499 Angstroms, in excellent agreement with values presented by Johnson et al for the (200) and (301) phases, respectively, of ß-C_3N_4. The absence of other discernible peaks associated with crystalline carbon nitride, especially in light of the good signal-to-noise ratio of the peaks, suggests that the films are grown with a preferred orientation. The middle trace in Fig. 2 is a diffraction pattern of carbon nitride similarly deposited onto a SiC on Si substrate. Strong agreement between the diffraction peaks of

films deposited onto different substrates lends further support to the ß-C_3N_4 assignment. No peaks assignable to alpha C_3N_4 or other known crystalline phases of carbon nitride are present in this data. Moreover, these diffraction patterns show no trace of a broad, low-angle (2 theta) signal commonly associated with amorphous material. Under these growth conditions, it is reasonable to suspect the existence of an epitaxial boundary layer at the growth interface due to the small dimensions of the NCN growth species. Such a boundary layer would not be detectable by x-ray diffraction.

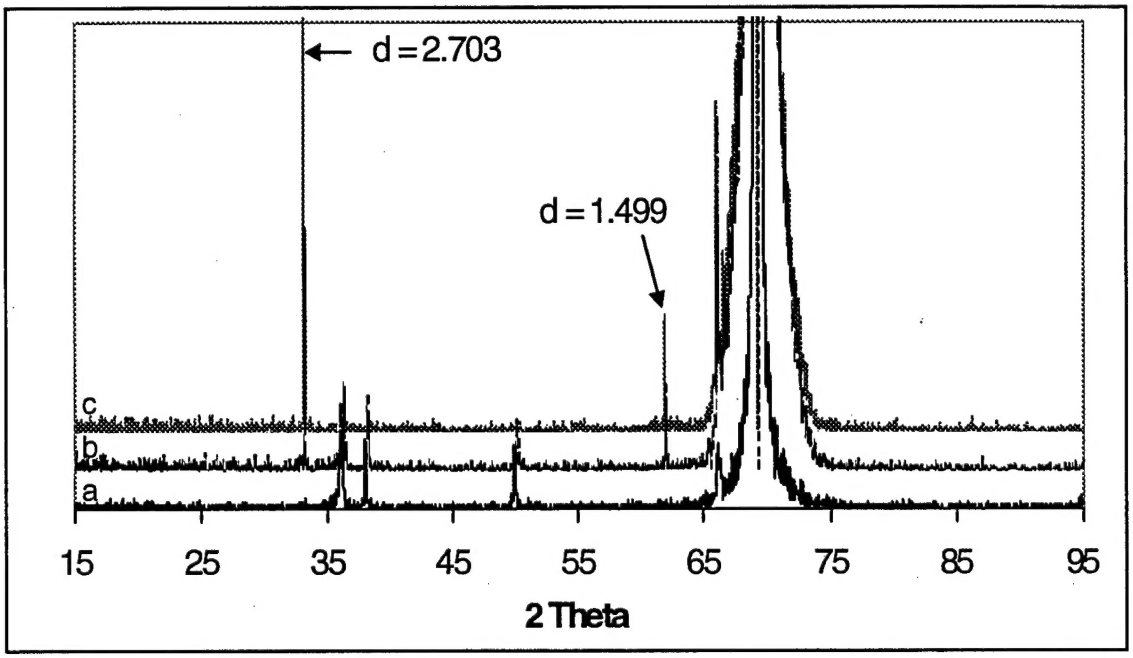

Figure 2. X-ray diffraction pattern of (a) an AlN film (2 μm) on a silicon substrate, (b) β-C_3N_4 deposited onto the substrate shown in (a), (c) β-C_3N_4 deposited onto SiC / Si.

Our results do not directly support the hypothesized incorporation of Si, an impurity reported to assist the growth of ß-C_3N_4, since similar data was obtained using

both AlN and SiC surfaces. Work in progress in this laboratory suggests that crystalline ß-C_3N_4 is also obtained using GaAs substrates while Johnson and coworkers[8] have reported crystalline growth of C_3N_4 (including both alpha and beta phases) on Ni substrates. It is reasonable to suspect that other heavy atom impurities may have a similar stabilizing influence on the growth of ß-C_3N_4. A critical test of this hypothesis will be growth of ß-C_3N_4 onto substrates composed solely of period 2 elements such as diamond or boron nitride.

Discussion

Many more studies are necessary to characterize these carbon nitride films with respect to hardness, nitrogen content, morphology and tribology. Success in the deposition of these films is likely owed to use of a "pre-bonded" CN precursor. In this light, it could be argued that other related precursor molecules may lead to films of still higher quality. For example, a fully coordinated carbon/nitrogen species in which the fundamental molecular structure is already sp^3 hybridized would have potential to further reduce the energy barrier necessary for crystalline growth.

By far, the greatest asset of the approach taken in this study is inherent simplicity. Damage to substrates is minimal, and the reagents used for deposition are inexpensive, reasonably facile, and amenable to handling in a vacuum flow system. Ultimate limitations in regard to growth rate, substrate dependence, and area scaling remain to be determined. Consequently, while there is much to learn concerning

production of crystalline ß-C_3N_4 by this reaction process, there is also considerable potential for near-term application of the products obtained.

Acknowledgements

This work was supported by contracts with the Anteon Corporation, the Air Force Wright Laboratory Materials Directorate, and the Air Force Office of Scientific Research.

References

1) A. Liu, M.L. Cohen, Science **245** (1989) 841.

2) D. Teter and R. Hemley, Science **271** (1996) 53.

3) Y.S. Gu, L. Q. Pan, X.R. Chang, Z.Z. Tian, J. Mater. Sci. Lett. **15** (1996) 1355.

4) Y. Chen, L. Guo, F. Chen, E.G. Wang: J. Phys, Condens. Matter **B** (1996) L685.

5) Y-A. Li, S. Xu, H-S Li, W-Y. Luo, J. Mater. Sci. Lett. **17** (1998) 31.

6) D. J. Johnson, Y. Chen, Y. He, R.H. Prince, Diam. Rel. Mat. **6** (1997) 1799.

7) D. Li, E. Cutiongco, Y-W Chung, M-S. Wong, W. Sproul, Surf. Coat. Tech. **68/69** (1994) 611 and L. Wan, R. F. Egerton, Thin Solid Films **279** (1996) 34.

8) J. Hu, P. Yang, C. Lieber, Phys. Rev. **B 57** (1997) 3158.

9) L.C. Chen, C. K. Chen, S. L. Wei, D. M. Bhusari, K. H. Chen, Y. F. Chen, Y. C. Jong, Y. S. Huang, Appl. Phys. Lett. **72** (1998) 2463.

10) D.J. Benard, C.J. Linnen, A.B. Harker, H.H. Michels, J. B. Addison, R. Ondercin, J. Phys. Chem. **B 31** (1998) 5943.

11) S. D. Ross, Inorganic Infrared and Raman Spectra (1972) 137.

1049 Camino Dos Rios
Thousand Oaks, CA 91360
(805) 373-4545 Fax (805) 373-4775

Rockwell Science Center

December 18, 1998 In Reply Refer To: SC71133.FTR

AFOSR/NL
Directorate of Chemistry
and Life Sciences
801 N. Randolph Street
Arlington, VA 22203-1977

Attention: Dr. Michael Berman, Room 732
F49620-97-C-0023

SUBJECT: Final Technical Report
Advanced Synthesis of Carbon Nitride
Contract No. F49620-97-C-0023

In accordance with requirements for Contract No. F49620-97-C-0023, enclosed is the Final Technical Report for the period 06/01/97 through 11/30/98.

ROCKWELL SCIENCE CENTER

David J. Benard

David J. Benard
Principal Investigator

DJB/mrw

enclosure

cc: Defense Technical Information Center
8725 John J. Kingman Road, Suite 0944
Fort Belvoir, VA 22060-6218

AFOSR/PKA
801 N. Randolph Street
Arlington, VA 22203-1977

DCMC Van Nuys
6230 Van Nuys Blvd.
Van Nuys, CA 91401-2713